Universidad del País Vasco Euskal Herriko Unibertsitatea

NAZIOARTEKO BIKAINTASUN CAMPUSA
CAMPUS DE EXCELENCIA INTERNACIONAL

UC UNIVERSIDAD DE CANTABRIA

POLITECNICO DI TORINO

Collegio di Ingegneria Chimica e dei Materiali

Corso di Laurea Magistrale

In Ingegneria Chimica e dei Processi Sostenibili

Tesi di Laurea Magistrale

Regeneration Strategies of Catalysts Structured in Ceramic Foams for Dry Reforming of Methane

Relatori

Stefania Specchia

Rubén López-Fonseca

Candidato

Giorgio Gandolfo

Marzo 2025

INDEX

1. LIST OF TABLES

2. LIST OF FIGURES

3. NOMENCLATURE

ATR .....Autothermal Reforming

CCS .....Carbon Capture and Storage

D .....Spacing between diffracted planes

DFT .....Density Functional Theory

DRM.....Dry reforming of methane

FWHM .....Full Width at Half Maximum

GHSV .....Gas Hourly Space Velocity

IPCC .....Intergovernmental Panel on Climate Change

K .....Form Factor

N .....Order of the diffraction peak

NAS.....National Academy of Sciences

PBQ .....PBQ type pre-column

RWGS.....Reverse water gas shift

SBA .....Santa Barbara Amorphous

SRM .....Steam reforming of methane

T .....Temperature, ºC

TCD.....Thermal Conductivity Detector

TPR.....Programmed temperature reduction

WGS .....Water gas shift

XCH4 .....Methane conversion

XCO2 .....Carbon dioxide conversion

XDR .....X-ray diffraction

YCO .....CO Performance

YH2 .....H Performance$_2$

Å .....Ångström, 10^{-10} m

B .....Width at half height corrected with instrumental contribution

Θ .....Angle of incidence, º

Λ .....Wavelength, nm

τ .....Average crystal size, nm

4. SUMMARY

This research focuses on the transition towards more sustainable energy sources due to the environmental problems caused by fossil fuels, which have been predominant since the Second Industrial Revolution and has led to exploration of alternatives such as solar, hydro, geothermal and wind energy, as well as waste-to-energy.

The study focuses on the production of syngas, particularly through steam reforming (SMR) and dry reforming of methane (DRM). SMR remains the most common industrial method of producing hydrogen, although it presents environmental challenges due to CO_2 emissions and high operating costs. On the other hand, DRM, which has recently gained attention, uses CO_2 and CH_4 to produce hydrogen and carbon monoxide, offering significant potential for CO_2 emissions reduction. However, it faces operational challenges such as carbon deposition on catalysts and the need for high temperatures. Current research focuses on developing more efficient and robust catalysts, as well as advanced reactor technologies to improve process efficiency and sustainability.

The objective is to optimize the H_2/CO ratio in the DRM by studying nickel and nickel/cobalt catalysts, and develop strategies to eliminate the coke deposited during the reaction, thus prolonging the useful life of the catalysts. Therefore, we proceed with the development of the project and the analysis of the main results obtained in the study of catalysts based on nickel and nickel-cobalt for the DRM reaction by integrating structural analysis by X-ray diffraction, hydrogen reduction characterizations (H_2-TPR) and evaluations of the catalytic activity both before and after catalyst regeneration with three different streams. This review aims to describe the structural properties of catalysts, their responses during reduction and regeneration, as well as their effectiveness in promoting the DRM reaction, highlighting the challenges and opportunities in improving catalytic performance for industrial applications.

The structural analysis of the catalysts was carried out using the X-ray diffraction (XRD) technique, revealing that the samples show a crystalline structure of nickel and cobalt oxides with a predominant phase of $NiAl_2O_4$ and $CoAl_2O_4$. This confirmed the presence of nanometric-sized crystals, which contribute to the increase in catalytic activity due to their high surface area and homogeneous dispersion of metals. Catalyst reduction was investigated using hydrogen reduction (H_2-TPR), which revealed that nickel was reduced at lower temperatures than cobalt, indicating greater ease in the formation of activated nickel metal for the DRM reaction. This process is crucial since metallic nickel is considered the main active site for the cleavage of C-H and C-O bonds.

During the catalytic activity study, it was observed that the monometallic nickel catalyst showed rapid initial deactivation, with methane and carbon dioxide conversions stabilized at around 35-40% after an adaptation period. The yields of CO were found to be higher than those of H_2, leading to a H_2/CO molar ratio that decreased with time due to competing reactions such as RWGS and coke formation, which inhibited the active sites. The introduction of cobalt into the Ni-Co catalysts improved the stability of the DRM reaction, with an H_2/CO ratio initially lower than the monometallic nickel catalysts, but more stable over time. This suggested a higher selectivity towards the desired reaction and a lower decomposition of the H_2/CO yield during the reaction.

The regeneration of the Ni catalyst was examined using three methods: O_2, H_2O, and H_2. Regeneration with O_2 did not show a significant increase in the H_2/CO ratio, indicating a good amount of coke oxidation and a decrease in efficiency in promoting the DRM reaction. As in the case of oxygen regeneration, H_2O regeneration did not show significant improvements in H_2/CO yield, showing a lower efficiency in removing coke from the active sites. Regeneration with H_2 was the most effective in restoring the H_2/CO ratio, indicating an effective reaction with coke to form methane and hydrogen that feed back into the DRM reaction. On the other hand, Ni-Co catalysts showed different behaviour compared to pure nickel catalysts during regeneration. While nickel benefited greatly from H_2 regeneration, Ni-Co showed a more consistent H_2/CO yield after regeneration, suggesting a partial but significant influence of cobalt on the reaction mechanisms.

In conclusion, the introduction of cobalt into Ni-Co catalysts was shown to improve selectivity toward the DRM reaction and limit coke formation, despite additional challenges in regeneration. Regeneration with O_2 proved to be effective in restoring the H_2/CO ratio for both catalysts, while H_2 showed greater benefit for the pure Ni catalyst. However, H_2O was found to be less effective at removing coke, suggesting that the choice of regeneration method can significantly affect catalyst performance. These results are crucial for the optimization of industrial processes based on methane catalysis, highlighting the importance of considering not only the catalytic performance during the reaction, but also the regeneration processes to improve the overall efficiency of the catalysts.

5 PREFACE

5.1. INTRODUZIONE

5.1.1. OBIETTIVO DELLA RICERCA

L'energia derivata dai combustibili fossili ha rappresentato per oltre un secolo il principale motore dello sviluppo industriale e sociale. Tuttavia, l'uso intensivo di queste risorse ha portato a un significativo impatto ambientale, in particolare attraverso l'aumento delle emissioni di gas serra, con conseguenze dirette sul cambiamento climatico. Già a partire dagli anni '50 e '60, gli scienziati hanno iniziato a studiare il fenomeno dell'effetto serra, evidenziando la correlazione tra l'aumento delle emissioni di CO_2 e il riscaldamento globale. Negli anni '70, questa tematica ha ricevuto crescente attenzione scientifica, culminando nel 1979 con il rapporto dell'Accademia Nazionale delle Scienze degli Stati Uniti, che ha sottolineato l'importanza di studiare il cambiamento climatico indotto dalle attività antropiche. Successivamente, la creazione dell'Intergovernmental Panel on Climate Change (IPCC) nel 1988 ha consolidato la base scientifica per l'analisi e la comunicazione delle problematiche legate al clima a livello globale.

Oltre alla CO_2, altri gas serra contribuiscono in modo significativo al riscaldamento globale, tra cui il metano (CH_4), il protossido di azoto (N_2O) e i gas fluorurati. Il metano, pur essendo presente in concentrazioni minori rispetto alla CO_2, possiede un potenziale di riscaldamento globale significativamente più elevato e deriva principalmente dall'agricoltura, dall'industria dei combustibili fossili e dalla gestione dei rifiuti. Il protossido di azoto, prodotto prevalentemente dall'uso di fertilizzanti agricoli, contribuisce anche alla riduzione dello strato di ozono. I gas fluorurati, utilizzati in diversi processi industriali, presentano un'elevata persistenza atmosferica e un impatto climatico particolarmente rilevante. L'azione combinata di questi gas provoca alterazioni nei modelli climatici globali, tra cui l'aumento della temperatura media terrestre, variazioni nelle precipitazioni, l'innalzamento del livello del mare e l'intensificazione degli eventi meteorologici estremi. Inoltre, l'acidificazione degli oceani, dovuta all'accumulo di CO_2 nell'atmosfera, rappresenta una minaccia significativa per gli ecosistemi marini. Di fronte a queste criticità, la comunità internazionale ha adottato una serie di misure volte alla riduzione delle emissioni di gas serra. Il Protocollo di Kyoto del 1997 e l'Accordo di Parigi del 2015 rappresentano due tappe fondamentali nel percorso verso la sostenibilità energetica.

Tuttavia, il raggiungimento di questi obiettivi richiede un impegno congiunto da parte di governi, industrie e cittadini, oltre allo sviluppo e all'implementazione di tecnologie innovative. Tra le soluzioni più promettenti emergono le fonti di energia rinnovabile, tra cui l'energia solare, eolica, idraulica e geotermica, che offrono alternative sostenibili ai combustibili fossili. Inoltre, la valorizzazione dei rifiuti attraverso processi di conversione energetica rappresenta un'opportunità rilevante per il recupero di energia. Un ruolo centrale è svolto nello sviluppo di tecnologie avanzate per la riduzione delle emissioni di gas serra e la produzione di energia pulita. Tra le soluzioni più innovative si annoverano la cattura e lo stoccaggio del carbonio (CCS), l'utilizzo di catalizzatori per la riduzione delle emissioni di N_2O nei processi industriali e lo sviluppo di nuovi materiali per la conversione energetica. Un'area di ricerca particolarmente promettente riguarda l'impiego dell'idrogeno come vettore energetico, in particolare l'"idrogeno verde", prodotto mediante processi che minimizzano l'impatto ambientale.

L'interesse per questa tecnologia ha portato a studi approfonditi sulle tecniche di cattura della CO_2 e sulla produzione di syngas, composto principalmente da CO e H_2, attraverso processi catalitici. La transizione verso un sistema energetico sostenibile rappresenta una sfida globale che richiede un approccio multidisciplinare e la collaborazione tra istituzioni, industria e ricerca. Grazie al suo ruolo nella progettazione e nell'ottimizzazione dei processi industriali, può fornire un contributo determinante nello sviluppo di soluzioni innovative per la riduzione delle emissioni di gas serra e la produzione di energia rinnovabile. L'adozione di tecnologie avanzate e l'investimento nella ricerca e nello sviluppo di nuovi materiali e processi saranno fondamentali per garantire un futuro energetico sostenibile e a basso impatto ambientale.

5.1.2. REFORMING A VAPORE E REFORMING A SECCO

Il reforming a vapore del metano rappresenta la tecnologia più comune per la produzione di syngas, composto principalmente da idrogeno e monossido di carbonio. Questo processo avviene a temperature comprese tra 700 °C e 1100 °C in presenza di un catalizzatore a base di nichel, facilitando la reazione tra metano e vapore acqueo. Storicamente, il reforming del metano è stato impiegato per la produzione di fertilizzanti e successivamente per soddisfare la crescente domanda di idrogeno nelle raffinerie e nell'industria chimica. Con il tempo, progressi nei materiali catalitici e nell'efficienza energetica hanno migliorato il processo, riducendone i costi operativi.

Negli ultimi anni, l'attenzione si è concentrata sull'integrazione del reforming con tecnologie di cattura e stoccaggio del carbonio (CCS) per ridurre le emissioni di CO_2. Tuttavia, il processo presenta ancora sfide ambientali e operative, tra cui l'elevato consumo energetico e la produzione di anidride carbonica come sottoprodotto. Per mitigare questi problemi, la ricerca sta esplorando alternative come il reforming secco del metano (DRM), che utilizza CO_2 come reagente, contribuendo alla riduzione dei gas serra.

Il reforming secco ha acquisito crescente interesse grazie al suo potenziale ambientale, sebbene la sua applicazione sia ostacolata dalla deposizione di carbonio nei catalizzatori e dalle alte temperature operative richieste. Innovazioni tecnologiche, tra cui lo sviluppo di catalizzatori più stabili e reattori avanzati, stanno migliorando l'efficienza del processo. Inoltre, l'integrazione del DRM con altre tecnologie di reforming e l'uso di energie rinnovabili stanno rendendo questa tecnologia più sostenibile e competitiva. Il syngas prodotto dal DRM può essere impiegato per la sintesi di combustibili liquidi, metanolo e prodotti chimici di base, rendendo questo processo un'opzione promettente per la valorizzazione di CO_2 e la produzione di energia pulita.

5.1.3. PROBLEMI NELL'APPLICAZIONE INDUSTRIALE

Il reforming secco del metano (DRM) presenta ancora sfide da superare per renderlo economicamente competitivo rispetto al reforming a vapore. Le alte temperature richieste, la gestione dei sottoprodotti e la durata dei catalizzatori sono aspetti critici da ottimizzare. La reazione, essendo lenta ed energivora, deve raggiungere l’equilibrio in tempi ridotti per un’efficace applicazione industriale. Inoltre, reazioni secondarie come la RWGS, la decomposizione del metano e la reazione di Boudouard influenzano il processo, portando alla

formazione di coke e alla disattivazione dei catalizzatori. Questo studio mira a ottimizzare il rapporto H_2/CO attraverso l'uso di catalizzatori a base di nichel e nichel/cobalto, sviluppando strategie innovative per ridurre la deposizione di coke e prolungare la durata dei catalizzatori.

5.2. REVISIONE BIBLIOGRAFICA

5.2.1. CATALIZZATORI HONEYCOMB VS SCHIUMA CERAMICA

Prima dell'implementazione del progetto pilota, è essenziale valutare le scelte relative ai catalizzatori e ai loro supporti, basandosi su studi scientifici recenti. Due strutture principali sono state analizzate: i monoliti e le schiume ceramiche a celle aperte. I monoliti, con una struttura geometrica regolare, garantiscono un buon flusso dei reagenti ma presentano difficoltà nel mantenere una temperatura uniforme e richiedono procedure complesse di preparazione. Le schiume ceramiche, invece, offrono un'elevata porosità, migliorando la diffusione dei reagenti, lo scambio termico e la resistenza meccanica.

Rispetto ai monoliti, le schiume ceramiche mostrano:

1. Maggiore attività catalitica a temperature più basse.
2. Maggiore stabilità e minore formazione di sottoprodotti.
3. Superficie catalitica più ampia grazie a cristalliti più piccoli.
4. Migliore adesione del catalizzatore.
5. Maggiore resistenza a stress meccanici e termici.
6. Distribuzione più uniforme del catalizzatore.

I test catalitici confermano che i catalizzatori su schiuma ceramica garantiscono un'attività superiore rispetto a quelli su monoliti, con una temperatura media più bassa e un profilo termico più uniforme. Pertanto, la schiuma a celle aperte rappresenta un'opzione preferibile per il DRM, grazie alla sua efficienza e stabilità.

5.2.2. DRM CON CATALIZZATORI A BASE DI NICHEL

Il nichel rappresenta il catalizzatore più studiato per il reforming secco del metano (DRM) grazie alla sua elevata attività catalitica, stabilità termica e costo relativamente basso rispetto ai metalli nobili. Tuttavia, la combinazione del nichel con altri elementi promotori si è rivelata una strategia efficace per migliorarne le prestazioni, in particolare per ridurre la deposizione di carbonio e aumentare la stabilità operativa.

I catalizzatori analizzati, ottenuti per coprecipitazione e successivamente calcinati a 800°C, hanno mostrato proprietà distinte:

- Ni-Mn: Caratterizzato dalla presenza della fase spinello $NiMn_2O_4$ con tracce di Mn_2O_3 e NiO, ha mostrato una scarsa dispersione del nichel sulla superficie. La sua riducibilità, evidenziata dalla riduzione di Mn_2O_3 a 390°C, non è stata sufficiente a garantire un'elevata selettività verso il syngas, risultando nel catalizzatore con la maggiore deposizione di coke.
- Ni-Co: La struttura predominante è Co_3O_4, con un'elevata attività catalitica e una riduzione del Co_3O_4 a Co^0 già a 405°C. Il catalizzatore ha mostrato un buon bilanciamento tra conversione del metano, selettività verso H_2 e minore tendenza alla formazione di coke rispetto a Ni-Mn.

- Ni-Cr: Il miglior catalizzatore tra quelli studiati, caratterizzato da una fase complessa con $NiCr_2O_4$, Cr_2O_3 e NiO. Ha mostrato una riducibilità più articolata, con transizioni multiple durante il processo. L'alta stabilità del sistema è stata attribuita alla presenza significativa di Cr_2O_3 (61%), che ha contribuito alla stabilizzazione dei siti attivi del nichel, migliorando sia l'attività catalitica che la resistenza alla formazione di coke.

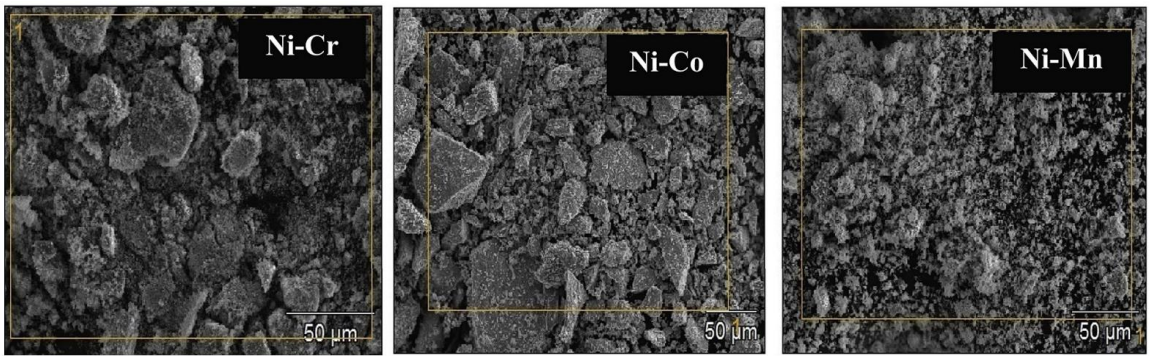

Figura I.- Microscopia Elettronica a scansione di catalizzatori diNi-Cr, Ni-Co e Ni-Mn.

L'ordine di efficienza catalitica osservato è stato Ni-Cr > Ni-Co > Ni-Mn, con Ni-Cr che ha fornito le migliori prestazioni in termini di conversione del metano e della CO_2, rapporto H_2/CO prossimo all'unità e minima deposizione di coke.

Problematiche associate all'uso del cromo: formazione di Cr^{6+}

Nonostante le eccellenti prestazioni catalitiche del Ni-Cr, recenti studi hanno sollevato preoccupazioni riguardo alla potenziale formazione di cromo esavalente (Cr^{6+}) durante il processo di sintesi e utilizzo del catalizzatore. Durante la calcinazione a temperature elevate (800°C), il cromo trivalente (Cr^{3+}) presente nel catalizzatore può subire un processo di ossidazione, generando specie di Cr^{6+} altamente tossiche (Goulas, 2017).

Il cromo esavalente è una delle forme più pericolose del cromo, noto per la sua elevata tossicità e cancerogenicità. Studi epidemiologici hanno evidenziato un forte legame tra l'esposizione a Cr^{6+} e gravi patologie, tra cui:

- Cancro ai polmoni e alla pelle (Gibb, 2000);
- Danni al sistema respiratorio e renale;
- Effetti mutageni e teratogeni.

La formazione di Cr^{6+} dipende da diversi fattori, come la temperatura di esercizio, la pressione e la presenza di ossigeno (Ukhurebor, 2021). Tuttavia, il rischio principale risiede nella possibilità che piccole quantità di cromo esavalente possano essere rilasciate nell'ambiente o accumulate nei residui del catalizzatore esausto, ponendo serie problematiche ambientali e di sicurezza per gli operatori.

Implicazioni per l'uso industriale e considerazioni sulla scelta del catalizzatore

Alla luce di queste evidenze, nonostante le prestazioni superiori di Ni-Cr nel DRM, il catalizzatore Ni-Co emerge come un'alternativa più sicura, sebbene meno efficiente. La sua elevata riducibilità e selettività verso H_2, insieme alla ridotta formazione di coke, lo rendono

un'opzione interessante per applicazioni industriali, soprattutto laddove la sicurezza e la sostenibilità ambientale siano criteri prioritari.

In conclusione, i risultati sperimentali dimostrano che le strutture di spinello possono rappresentare precursori promettenti per catalizzatori DRM altamente attivi, ma è necessaria una valutazione attenta delle implicazioni ambientali legate alla stabilità chimica e alla tossicità dei materiali impiegati. Future ricerche dovrebbero approfondire la reale fase attiva del cromo nei catalizzatori Ni-Cr e individuare strategie per minimizzare la formazione di Cr^{6+}, garantendo così un utilizzo sicuro e sostenibile nel lungo periodo.

5.2.3. DRM CON CATALIZZATORI A BASE DI COBALTO

I catalizzatori a base di cobalto hanno registrato un rapido sviluppo negli ultimi anni, dimostrando una particolare superiorità grazie alle loro caratteristiche chimico-fisiche. La ricerca si concentra sempre più sui catalizzatori bimetallici a base di cobalto, che rappresentano una sfida a lungo termine. Diversi metalli di transizione, come Pt, Ru, Rh e Ni, sono stati utilizzati come promotori per migliorare le prestazioni catalitiche. Gli studi evidenziano l'importanza di fattori quali lo stoccaggio dell'ossigeno, la dispersione attiva del metallo, l'interazione metallo-supporto e la modifica delle proprietà chimiche superficiali per ottimizzare l'attività catalitica (Sun, 2024).

L'aggiunta di metalli nobili come il Pt ai catalizzatori a base di Co migliora la forza di legame delle specie di ossigeno, aumentando l'attività catalitica. Il Pt, in particolare, favorisce la riducibilità del Co attraverso l'effetto spillover dell'idrogeno, abbassando la temperatura di riduzione e migliorando la stabilità del catalizzatore. Studi condotti su sistemi Co/TiO_2-Al_2O_3 modificati con Pt hanno mostrato che una composizione ottimale di 5% Co e 0,5% Pt garantisce elevate prestazioni nella reazione DRM. Inoltre, la formazione di leghe Pt-Co favorisce una maggiore attività catalitica rispetto ai catalizzatori monometallici. Studi DFT e cinetici hanno confermato che la presenza di Pt riduce la barriera di attivazione del legame C-H, limitando la formazione di coke (Sun, 2024).

Il Ru rappresenta un'alternativa economicamente vantaggiosa al Pt per migliorare le prestazioni dei catalizzatori Co. La ricerca condotta su sistemi Co/SBA-15 ha evidenziato che un contenuto ottimale di 5% Co e 0,1% Ru migliora significativamente l'attività catalitica. Il Ru si localizza principalmente sulla superficie esterna dei pori, mentre il Co occupa sia l'interno che l'esterno, ottimizzando la distribuzione del metallo attivo. L'effetto spillover dell'idrogeno promuove la riduzione del Co, riducendo la temperatura di riduzione complessiva. Tuttavia, oltre un carico dello 0,14% in peso di Ru, non si osservano ulteriori miglioramenti. La combinazione Co-Ru aumenta la resistenza all'ossidazione e alla formazione di coke, rendendo il catalizzatore più stabile (Sun, 2024).

Il Rh migliora la struttura elettronica del catalizzatore e ottimizza la dissociazione della CO_2 in presenza di CH_4, migliorando la reattività nella reazione DRM. Studi comparativi su sistemi Co/Al2O3 promossi con Ni, Rh e Ru hanno dimostrato che il Rh garantisce le migliori prestazioni catalitiche a diverse temperature. Questo comportamento è attribuibile alla formazione di spinelli nanocristallini di alluminato di cobalto con eccellenti proprietà redox. La maggiore efficienza di dissociazione della CO_2 nei catalizzatori Rh-Co è correlata alla stabilizzazione delle specie reattive e alla minimizzazione della formazione di coke. Tuttavia,

il costo elevato del Rh limita la sua applicazione su larga scala, rendendo necessaria un'ottimizzazione del contenuto di metallo nobile (Sun, 2024).

L'aggiunta di Ni ai catalizzatori Co migliora la reattività della decomposizione di CH_4 e CO_2. I catalizzatori Co-Ni presentano migliori proprietà redox rispetto ai sistemi monometallici. Il Co, grazie alla sua elevata affinità con l'ossigeno attivo, limita la formazione di coke, migliorando la stabilità del catalizzatore. La CO_2 ossida parzialmente il Co a CoO, che viene poi ridotto a Co0 in presenza di CHx. Il rapporto molare Ni/Co influenza significativamente le proprietà del catalizzatore: un rapporto 9:1 garantisce un'ottima stabilità nella reazione DRM. Tuttavia, un eccesso di Co può ridurre l'attività catalitica e aumentare la formazione di coke. L'aggiunta di Co favorisce anche la riduzione della dimensione delle particelle di Ni, migliorando la stabilità del catalizzatore e limitando la sinterizzazione del metallo attivo. La lega Ni-Co ottimizza la densità elettronica del Ni, inibendo la completa dissociazione del CH_4 e facilitando l'adsorbimento e l'attivazione della CO_2, migliorando così la stabilità del catalizzatore (Sun, 2024).

I catalizzatori a base di Co presentano eccellenti proprietà catalitiche nella reazione DRM, inclusa un'elevata attività, stabilità e resistenza alla formazione di coke (Wang, 2022). Tuttavia, rimangono alcune criticità nello sviluppo di tali catalizzatori. La ricerca futura dovrebbe approfondire i meccanismi di reazione e sviluppare nuovi sistemi catalitici con supporti porosi per migliorare la dispersione del metallo attivo e la stabilità del catalizzatore. Un approccio promettente è lo sviluppo di metodi per la dispersione atomica del metallo attivo, che potrebbe aumentare il numero di siti attivi e migliorare l'efficienza catalitica. Inoltre, la ricerca dovrebbe concentrarsi sulla reazione DRM a bassa temperatura per ottimizzare il risparmio energetico e ridurre l'impatto ambientale (Chen, 2023).

5.3. SVILUPPO SPERIMENTALE

5.3.1. SINTESI CATALITICA

Il catalizzatore è stato sintetizzato attraverso il percorso di sintesi in soluzione (SCS). Seguendo questa metodologia, sono state preparate soluzioni con concentrazioni aggiustate di $Ni(NO_3)_2 \cdot 6H_2O$, $Al(NO_3)_3 \cdot 9H_2O$ e $Co(NO_3)_2 \cdot 6H_2O$, insieme alla glicina. In tutte le soluzioni, la concentrazione di nitrati è stata fissata a 4 mol $^{L-1}$. Allo stesso modo, per ottenere il catalizzatore monometallico Ni, il rapporto molare Ni/Al della soluzione è stato fissato a 0,5; mentre per ottenere il catalizzatore Ni-Co bimetallico è stato fissato il rapporto molare (Ni+Co)/Al a 0,5 e il rapporto molare Ni/Co a 1.

In questo metodo di sintesi, la glicina ($C_2H_5NO_2$) è stata utilizzata come combustibile ossidato da nitrati in soluzione. L'uso della glicina nella sintesi del catalizzatore attraverso il metodo SCS offre diversi vantaggi chiave. La glicina agisce come un combustibile che reagisce con i nitrati, favorendo una combustione vigorosa che genera abbastanza calore da formare ossidi metallici. Questo processo permette di ottenere catalizzatori con elevata purezza, omogeneità chimica e buona distribuzione granulometrica. Inoltre, il metodo è semplice, efficace e rispettoso dell'ambiente (Carbos, 2018). La quantità di glicina da aggiungere a ciascuna soluzione è stata calcolata come punto stechiometrico, secondo le seguenti reazioni:

$$Ni(NO_3)_2 + \frac{10}{9} C_2H_5NO_2 \rightarrow NiO + \frac{20}{9} CO_2 + \frac{25}{9} H_2O + \frac{14}{9} N_2 \quad \text{(I)}$$

$$Al(NO_3)_2 + \frac{5}{3} C_2H_5NO_2 \rightarrow \frac{1}{2} Al_2O_3 + \frac{10}{3} CO_2 + \frac{25}{6} H_2O + \frac{7}{3} N_2 \quad \text{(II)}$$

$$Co(NO_3)_2 + \frac{28}{27} C_2H_5NO_2 \rightarrow \frac{1}{3} Co_3O_4 + \frac{56}{27} CO_2 + \frac{70}{27} H_2O + \frac{17}{11} N_2 \quad \text{(III)}$$

Una volta preparate le soluzioni, il passo successivo è stato quello di metterle in contatto con il supporto precedentemente selezionato. In questo caso sono state utilizzate schiume ceramiche a celle aperte α-Al_2O_3, con dimensioni di 10 mm di lunghezza e 8 mm di diametro. Ogni blocco di schiuma è stato immerso in una delle due soluzioni per 5 minuti, dopodiché l'eccesso è stato rimosso con aria compressa. Le schiume impregnate sono state poi poste in un forno a 300°C per 30 minuti per avviare il processo di combustione. Questo processo di impregnazione e combustione è stato ripetuto per un totale di 5 volte, fino a raggiungere un carico totale in fase attiva di circa il 10-11% del peso totale della schiuma. Infine, le schiume sono state poste in un forno a 850 °C per 4 ore, in modo da formare gli spinelli $NiAl_2O_2$ e $CoAl_2O_4$ attraverso la reazione allo stato solido degli ossidi NiO, Al_2O_3 e Co_3O_4 formatisi durante i cicli di combustione.

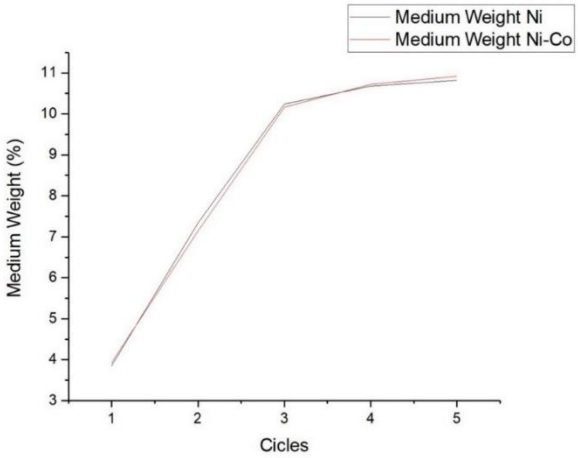

Figura II.- Evoluzione della carica metallica delle schiume con il numero di cicli SCS.

Il grafico nella Figura II illustra l'aumento percentuale medio del peso dei catalizzatori impregnati di nichel e nichel-cobalto. Come si può vedere dopo il terzo ciclo, la percentuale in peso aumenta di una quantità minore, questo perché lo strato catalitico depositato assorbe meno soluzione rispetto alla superficie della schiuma ceramica pulita, il che riduce la massa dello strato catalitico depositato nei cicli successivi.

5.3.2. DIFFRAZIONE A RAGGI X (XRD)

La cristallografia dei catalizzatori è un aspetto cruciale per comprenderne le proprietà e il funzionamento. Per valutare con precisione la dimensione media dei cristalli e identificare le fasi cristalline presenti nei campioni, è indispensabile la tecnica della diffrazione a raggi X (XRD). Questa metodologia non solo consente una caratterizzazione strutturale dettagliata dei materiali catalitici, ma fornisce anche informazioni fondamentali sulla loro organizzazione atomica e sulla dimensione dei domini cristallini. Attraverso l'analisi del pattern di diffrazione, è possibile dedurre la disposizione interna degli atomi e le eventuali imperfezioni presenti nella struttura cristallina, offrendo una comprensione approfondita che è essenziale per ottimizzare le prestazioni del catalizzatore.

Il protocollo sperimentale dell'analisi è stato effettuato presso il SGIker General Research Services dell'Università dei Paesi Baschi UPV/EHU. Le analisi sono state eseguite su un diffrattometro PANalytical X'Pert PRO dotato di un monocromatore sintonizzato perα la radiazione Cu K (λ = 1,5406 Å) e di un filtro Ni. I diffrattogrammi sono stati effettuati tra le posizioni 2θ = 5-80°.

5.3.3. RIDUZIONE A TEMPERATURA PROGRAMMATA CON H_2 (H_2-TPR)

La tecnica di riduzione programmata della temperatura (TPR) fornisce informazioni sulla reattività dei catalizzatori in condizioni riducenti. Durante il test, un catalizzatore viene esposto a un gas riducente, tipicamente idrogeno, mentre la temperatura aumenta gradualmente. Questo processo permette di analizzare la riduzione dei composti presenti sulla superficie del catalizzatore, reazioni che sono generalmente esotermiche e rilasciano calore.

Nel caso della riduzione con idrogeno (H_2-TPR), un catalizzatore viene esposto a una miscela del 5% di H_2 in argon, con un incremento controllato della temperatura. La concentrazione di idrogeno nel flusso di uscita viene monitorata tramite un rivelatore di conducibilità termica (TCD), permettendo di determinare la quantità totale di idrogeno consumata, la temperatura alla quale avviene la riduzione e il grado di riduzione del campione. Questo consente di dedurre lo stato ossidativo medio del materiale prima della riduzione (Chin, 1993).

Gli esperimenti H_2-TPR sono stati condotti utilizzando un dispositivo Micrometrics Autochem II. Per ogni analisi, 0,1 g di campione sono stati inseriti in un reattore a forma di U in quarzo, supportati da lana di quarzo. Le analisi sono state effettuate con una rampa di temperatura di 10 °C/min fino a 950 °C. Per evitare alterazioni nelle misure di conducibilità dovute all'acqua generata, è stata utilizzata una trappola fredda mantenuta a -10 °C tramite un sistema a base di isopropanolo raffreddato con azoto liquido (Ertl, 2008).

5.3.4. STUDIO DELL'ATTIVITÀ CATALITICA

L'attività catalitica dei materiali sintetizzati è stata analizzata in un reattore a letto fisso PID Eng&Tech, dotato di un reattore tubolare in quarzo con un diametro di 9 mm operante a pressione atmosferica. Il sistema di riscaldamento del reattore è costituito da un forno cilindrico con resistenza elettrica, mentre la temperatura è misurata e controllata tramite una termocoppia multipunto di tipo K.

L'alimentazione del gas è regolata da flussometri di massa, e i gas in uscita vengono analizzati mediante un cromatografo Agilent 990 microGC. Questo sistema è composto da due canali: il canale A, con una colonna a setaccio molecolare da 10 m e precolonna PBQ da 3 m per l'analisi di gas permanenti come H_2, N_2, O_2 e CO, e il canale B, con una colonna PPQ da 10 m per l'analisi di CH_4 e CO_2. Un raffreddatore di Peltier rimuove l'acqua generata durante la reazione per prevenire interferenze nell'analisi cromatografica.

L'attività catalitica è stata studiata seguendo lo stesso protocollo per tutti i campioni. Prima della reazione, i precursori catalitici sono stati ridotti in situ con un flusso di H_2 al 5% in azoto a 850 °C per 2 ore. I test di reazione sono stati condotti a 650 °C, con una portata totale di 800 cm^3/min di una miscela gassosa composta da 10% CH_4, 10% CO_2 e 80% N_2 per una durata di 72 ore. La velocità spaziale media era pari a 96000 h^{-1}, garantendo condizioni ottimali per l'analisi della stabilità e dell'efficienza catalitica dei materiali testati.

5.4. RISULTATI

5.4.1. CARATTERIZZAZIONE DEI PRECURSORI CATALITICI

L'analisi della struttura dei supporti ceramici mediante diffrazione di raggi X ha evidenziato la presenza di più fasi cristalline, tra cui alfa-Al_2O_3, mullite, cristobalite e cordierite. Questi materiali conferiscono stabilità meccanica e termica al supporto catalitico, migliorando la dispersione del catalizzatore e garantendo una maggiore resistenza agli shock termici e all'usura. Inoltre, l'uso di materiali ceramici relativamente economici contribuisce alla riduzione dei costi senza compromettere le prestazioni.

Le analisi XRD sui precursori dei catalizzatori hanno confermato la presenza di una fase spinello, con una dimensione media dei cristalli di 15 nm nel precursore monometallico di Ni e di 22 nm in quello bimetallico Ni-Co. Dopo la riduzione, i picchi dello spinello scompaiono e compaiono segnali associati ai cristalli metallici di Ni e Ni-Co, con dimensioni rispettivamente di 22 nm e 24 nm. L'incremento della dimensione dei cristalli è più evidente nel catalizzatore monometallico, mentre la presenza di cobalto sembra limitare questo fenomeno grazie alla formazione di leghe stabili che riducono la crescita dei cristalli.

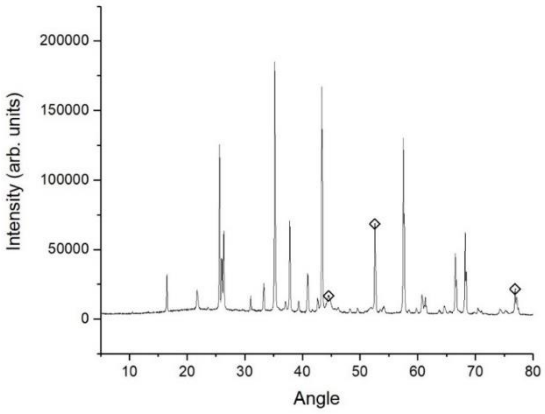

Figura III.- Diffrattogramma a raggi X del catalizzatore di Ni.

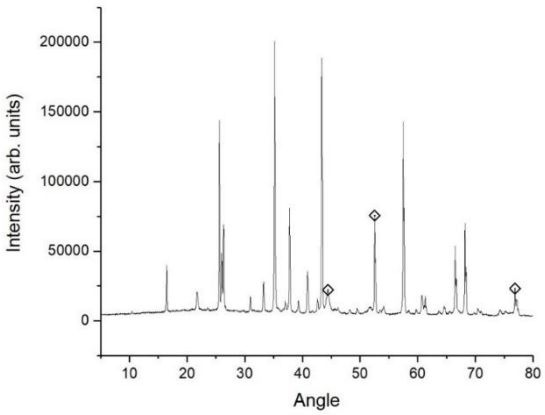

Figure IV.- Diffrattogramma a raggi X del catalizzatore di Ni-Co

L'analisi TPR ha permesso di studiare il comportamento redox dei precursori catalitici. I risultati hanno mostrato due principali contributi al consumo di idrogeno: uno a bassa temperatura (350-450 °C), attribuito alla riduzione degli ossidi segregati di NiO e Co_3O_4, e uno ad alta temperatura (>550 °C), associato alla riduzione degli alluminati di nichel e cobalto. La maggiore intensità del contributo ad alta temperatura nei precursori bimetallici indica che l'incorporazione di cobalto favorisce la formazione di alluminati, con una percentuale di nichel convertito in alluminato del 78% nel precursore monometallico e dell' 86% in quello bimetallico.

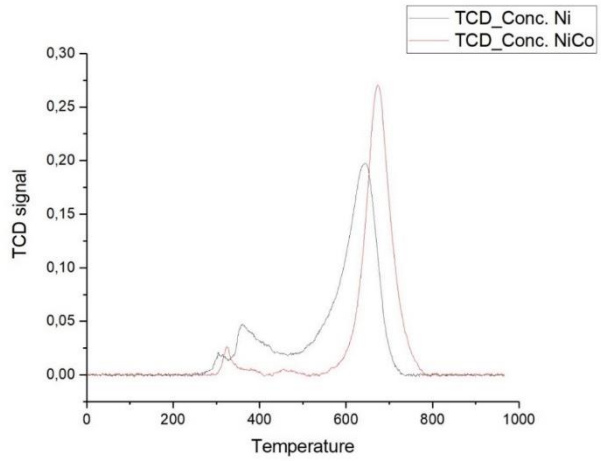

Figura V.- Profili TPR dei precursori catalitici.

Questi risultati suggeriscono che l'aggiunta di cobalto nei catalizzatori a base di nichel influisce positivamente sulla stabilità strutturale e sulle proprietà redox, migliorando la resistenza alla crescita dei cristalli e promuovendo la formazione di fasi alluminato più stabili.

5.4.2. RISULTATI DELLA REAZIONE SENZA RIGENERAZIONE

L'attività catalitica delle schiume di nichel e nichel-cobalto è stata studiata per la reazione di reforming secco del metano (DRM) a 650 °C per 72 ore, monitorando la conversione dei reagenti e il rapporto molare H_2/CO nei prodotti.

Per il catalizzatore monometallico a base di nichel, le conversioni iniziali di CH_4 e CO_2 erano rispettivamente del 40% e 45%, ma una rapida disattivazione nelle prime 10 ore ha portato a una stabilizzazione attorno al 35-40%. Le rese dei prodotti hanno seguito un andamento simile, con la produzione di CO superiore a quella di H_2. Il rapporto H_2/CO è diminuito progressivamente da 0,72 a 0,65, indicando un incremento delle reazioni secondarie, tra cui la reazione inversa di Water-Gas Shift (RWGS) e la formazione di coke, che inibiscono i siti attivi e riducono l'efficienza catalitica.

Per il catalizzatore bimetallico Ni-Co, le conversioni di CH_4 e CO_2 sono risultate più stabili nel tempo, suggerendo che la presenza di cobalto ha un effetto stabilizzante sulla reazione. Tuttavia, il rapporto H_2/CO è sceso più marcatamente da 0,69 a 0,57. Ciò indica che, sebbene il cobalto migliori la selettività della reazione DRM rispetto al nichel puro, esso subisce una maggiore riduzione nella produzione di H_2 a causa della deposizione di coke nei siti attivi.

In generale, i risultati dimostrano che il catalizzatore Ni-Co è più resistente alla disattivazione rispetto al nichel monometallico, ma entrambi i catalizzatori sono soggetti alla formazione di coke, che compromette l'efficienza del processo. Per migliorare la stabilità operativa e mantenere l'attività catalitica nel tempo, è necessaria una strategia di rigenerazione per rimuovere il coke accumulato e ripristinare i siti attivi.

5.4.3. RISULTATI CON LA RIGENERAZIONE

Sono state valutate tre strategie di rigenerazione per rimuovere il coke depositato sui catalizzatori: trattamento con ossigeno (O_2), con vapore acqueo (H_2O) e con idrogeno (H_2).

Per il catalizzatore monometallico al nichel, la rigenerazione con O_2 ha rimosso il coke ma ha anche danneggiato il catalizzatore, portando a una riduzione delle conversioni di CH_4 e CO_2 e delle rese di H_2 e CO. Analogamente, la rigenerazione con vapore acqueo ha causato una diminuzione del rapporto molare H_2/CO e delle prestazioni catalitiche, sebbene in misura minore rispetto all'ossigeno. Al contrario, il trattamento con H_2 ha permesso di rimuovere il coke senza compromettere la struttura del catalizzatore, mantenendo stabili le conversioni e aumentando il rapporto H_2/CO.

Per il catalizzatore bimetallico Ni-Co, la rigenerazione con O_2 ha migliorato significativamente le conversioni di CH_4 e CO_2 e la resa di H_2, suggerendo un effetto positivo del cobalto, che impedisce la riossidazione del nichel. La rigenerazione con vapore acqueo, invece, ha portato a una drastica riduzione delle prestazioni, risultando ancora meno efficace rispetto al catalizzatore monometallico. La rigenerazione con H_2 ha mantenuto inalterati i parametri di reazione, senza migliorare né peggiorare le prestazioni.

Nel complesso, per il catalizzatore Ni, solo la rigenerazione con H_2 ha migliorato il rapporto H_2/CO, mentre per Ni-Co, l'ossigeno si è rivelato il metodo più efficace. In entrambi i casi, il trattamento con vapore acqueo si è dimostrato dannoso per la stabilità e l'attività catalitica.

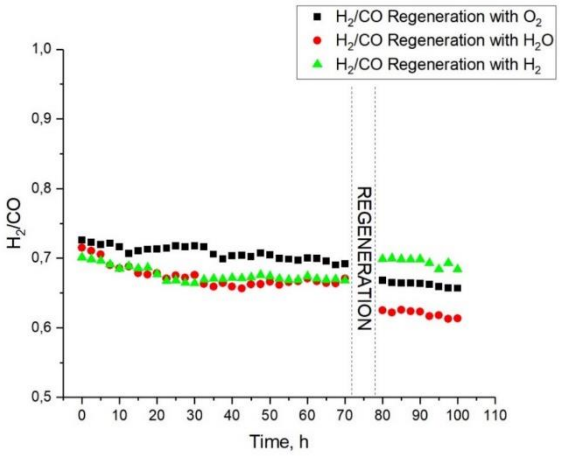

Figura VI.- Confronto del rapporto molare H_2/CO del catalizzatore Ni per le tre strategie di rigenerazione.

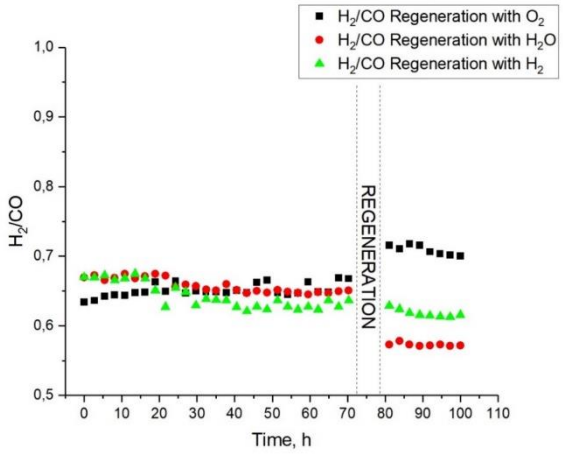

Figura VII.- Confronto del rapporto molare H_2/CO del catalizzatore Ni-Co per le tre strategie di rigenerazione.

5.5. CONCLUSIONI

L'analisi del comportamento dei catalizzatori a base di nichel e nichel-cobalto dopo il processo di rigenerazione ha evidenziato differenze sostanziali dovute alle loro proprietà chimiche. Il cobalto, grazie alla sua elevata affinità per l'ossigeno, tende a formare ossidi (CoO, Co_3O_4) che favoriscono le reazioni di ossidazione del carbonio, altamente esotermiche e favorevoli alla produzione di metano. Il nichel, invece, è particolarmente selettivo nella metanazione, grazie alla sua capacità di adsorbire e dissociare efficacemente idrogeno e carbonio, facilitando la formazione di intermedi stabili come CHx.

I risultati sperimentali mostrano che la rigenerazione con idrogeno ha ripristinato efficacemente i siti attivi del catalizzatore monometallico di nichel, aumentando il rapporto H_2/CO. Al contrario, la rigenerazione con ossigeno ha portato alla formazione di ossidi di nichel, avvelenando i siti attivi e riducendo la capacità del catalizzatore di promuovere la reazione. Per il catalizzatore bimetallico Ni-Co, la rigenerazione con idrogeno ha mantenuto stabile il rapporto H_2/CO, suggerendo un'interazione tra i due metalli che ha impedito un recupero completo dell'attività del nichel. La rigenerazione con ossigeno, invece, ha aumentato significativamente il rapporto H_2/CO, indicando che il cobalto ha favorito l'ossidazione del coke e migliorato la disponibilità di carbonio per la reazione.

In conclusione, il nichel puro ha mostrato prestazioni ottimali con la rigenerazione a idrogeno, mentre la combinazione Ni-Co ha beneficiato maggiormente della rigenerazione con ossigeno. Questi risultati suggeriscono la necessità di ottimizzare le condizioni di rigenerazione per migliorare l'efficienza e la stabilità dei catalizzatori. Studi futuri dovrebbero approfondire l'interazione tra nichel e cobalto e valutare nuove formulazioni catalitiche per massimizzare la selettività della reazione e la resistenza alla deattivazione.

6. INTRODUCTION

6.1. OBJECTIVE OF THE RESEARCH

Fossil fuel energy has fueled the world since the Second Industrial Revolution for nearly 150 years. This energy is present in our homes, in our transportation, and throughout our daily lives. Unfortunately, however, such a powerful energy medium is also responsible for many problems for the Earth's climate.

One of the first signs of this problem dates back to the 1950s and 1960s, when some scientists began studying the greenhouse effect and hypothesized that increased CO_2 emissions could lead to significant climate change. Subsequently, it was in the 1970s that this topic received more attention, especially after the publication of some scientific studies highlighting the link between CO_2 emissions and global warming (NAS, 1979). One of the turning points was the 1979 report of the United States National Academy of Sciences, titled "Understanding Climate Change: An Agenda for Action," which emphasized the importance of studying human-caused climate change, including CO_2 emissions from fossil fuels (Arrhenius, 1896). In the years since, scientific and public attention to the link between fossil fuel use and CO_2 emissions has grown steadily, culminating in the formation of the Intergovernmental Panel on Climate Change (IPCC) in 1988, which has played a key role in the analysis and communication of climate change science globally (IPCC, 2014).

Today, climate change and the increasingly emerging scarcity of fossil fuel resources are pushing governments and various global entities to reduce the consumption of carbon sources and to develop technologies that meet the economic and energy needs of nations in such a way that they constitute the least possible environmental impact. This technological advance has led to the study of solutions capable of taking advantage of the solar energy of our star, the hydraulic energy of the sea, the geothermal energy of the subsoil and the wind energy of the winds, excellent green alternatives to the consumption of petroleum derivatives (Hoffert, 2002). In addition, through the study of waste, important energy alternatives have been identified. Whether they are organic, plastic or cellulosic, their correct transformation can produce energy (UNFCCC, 2015).

An in-depth analysis of climate change dynamics revealed the importance of considering not only CO_2, but also other greenhouse gases such as methane (CH_4), nitrous oxide (N_2O), and fluorinated gases. Methane, for example, has a much greater global warming power than CO_2, although it is present in smaller quantities in the atmosphere. Methane emissions come mainly from agriculture, the fossil fuel industry, and waste management (IEA, 2020). N_2O, produced primarily by the use of agricultural fertilizers, has a significant impact on global warming and also contributes to the destruction of the ozone layer. In addition, fluorinated gases, which are used in various industrial applications, have an extremely high global warming potential and a long atmospheric lifetime.

The combined effect of these greenhouse gases and their interactions with the Earth's climate system leads to an increase in global average temperature, changes in precipitation patterns, sea level rise, and an increase in the frequency and intensity of extreme weather events. These changes have a significant impact on biodiversity, agriculture, water availability and human health. Another crucial aspect is ocean acidification, caused by increased atmospheric CO_2 concentrations (Solomon, 2009). This phenomenon has devastating consequences on marine

ecosystems, influencing the lives of numerous species and altering their delicate ecological balance.

To address these challenges, the international community has adopted several agreements and treaties, including the 1997 Kyoto Protocol and the 2015 Paris Agreement, which aim to reduce greenhouse gas emissions and limit global temperature rise (UNFCCC, 2015). These efforts require cooperation among nations, industries, and citizens to adopt sustainable practices and technologies with low environmental impact. In this context, chemical engineering plays a key role in the development of innovative processes and technologies for the reduction of greenhouse gas emissions and the production of sustainable energy. The implementation of advanced technologies such as carbon capture and storage (CCS), the use of catalysts to reduce N_2O emissions in industrial processes, and the development of new materials for clean energy production are just a few of the areas of research where chemical engineering can make a difference.

In conclusion, the transition to a sustainable energy future requires a global and interdisciplinary effort, in which chemical engineering plays a crucial role in providing innovative and sustainable solutions to address the challenges of climate change and the management of energy resources (Gielen, 2019).

In this chaos of energy resources competing with fossil fuels, some research has focused on the use of hydrogen as an alternative energy source (Armor, 1999). It is precisely the interest in this "green hydrogen" that has led research to focus on CO_2 capture technologies, which aim to produce syngas (syngas) composed mainly of CO and H_2 (Rostrup-Nielsen, 1984).

6.2. STEAM REFORMING AND DRY REFORMING

The most common industrial application for syngas production is natural gas steam reforming. Methane vapor reforming is a chemical process used to produce hydrogen (H_2) and carbon monoxide (CO) from methane (CH_4), which is the main component of natural gas. This process is carried out at high temperatures and with the presence of water vapor (H_2O) and a suitable catalyst. Methane steam reforming is a key technology for the production of syngas. This process takes place at high temperatures, typically between 700 °C and 1100 °C, and requires the presence of a catalyst, usually nickel-based, to facilitate the reaction between methane and water vapor.

The reforming of methane vapours has historical roots dating back to the early twentieth century, with the development of the first catalytic reforming processes. Initially, this process was mainly used to produce syngas for the chemical industry and for the production of fertilizers. The adoption of nickel-based catalysts has been a significant advance, improving the efficiency and selectivity of the process. In the 1950s and 1960s, as demand for hydrogen for oil refining and ammonia production increased, the steam reforming process saw further progress. Therefore, more efficient reactors and heat management systems have been introduced to optimize energy efficiency. In addition, the development of new catalytic materials and a deeper understanding of reaction dynamics have reduced operating costs and increased catalyst life.

Over the past few decades, methane vapor reforming has continued to evolve with the introduction of advanced technologies and hybrid processes. For example, integration with carbon capture and storage (CCS) has become an increasingly common practice to reduce CO_2 emissions associated with the process. In addition, advanced catalysts and innovative reactor systems, such as membrane reactors, have been developed that further improve process efficiency and enable purer hydrogen production.

Despite the advances, methane vapor reforming continues to present challenges, especially with regard to CO_2 emissions. To address these issues, research is focusing on more sustainable alternatives, such as solar-powered renovation and electrolysis of water powered by renewable sources. In addition, the development of low-temperature reforming technologies and the optimization of gas purification processes are areas of great interest.

In addition to the production of syngas, methane vapor reforming is used in numerous industries. The hydrogen produced is used in refineries for hydrodesulphurization processes, in the production of ammonia for fertilizers, and in the synthesis of methanol. In addition, with the emergence of the hydrogen economy, the role of steam reforming could be further expanded, acting as a bridge to a more sustainable energy transition (Rostrup-Nielsen, 2011).

The methane steam reforming process is carried out in two main phases:

1. Steam reforming reaction:

$$CH_4 + H_2O \rightarrow CO + 3H_2 \quad (1)$$

2. Water Gas Displacement Reaction (WGS):

$$CO + H_2O \rightarrow CO_2 + H_2 \quad (2)$$

In this process, methane reacts with water vapor to produce hydrogen and carbon monoxide. Subsequently, the carbon monoxide produced is transformed into carbon dioxide plus hydrogen through the second reaction.

However, as mentioned above, steam reforming presents a number of problems that in some cases lead to a re-evaluation of the process. Firstly, it produces significant amounts of CO_2 as a by-product, and although hydrogen is the main desired product, the production of large amounts of CO_2 can be problematic from an environmental point of view since, as mentioned above, its contribution to the greenhouse effect and climate change is very significant (Balasubramanian, 1999). For this reason, it is necessary to remove CO_2 from by-products and therefore it is inevitable to face the additional costs related to the capture and purification of this gas to reduce emissions into the atmosphere. In addition to this, steam reforming requires high temperatures (around 750-900 °C) and significant pressures to achieve it efficiently. These operating conditions require investment in specialized and expensive equipment and increase process and energy costs (Choi, 2003). Therefore, these overhead operating costs mean that steam reforming is not considered such a beneficial technology.

In this way, a possible alternative to this strategy is dry methane reforming (DRM). Dry methane reforming was first explored several decades ago, but has only recently begun to receive significant attention due to its environmental potential (Song, 2006). Another promising strategy is oxy-steam reforming (OSR), which combines water vapor with a controlled amount of oxygen to improve energy efficiency and reduce carbon formation on catalysts. This process

optimizes the system's thermal balance and allows for a more adjustable H_2/CO ratio, making it suitable for various industrial applications (Specchia, 2017). Among the alternatives to steam reforming, DRM stands out for its ability to directly use CO_2 as a reactant, potentially reducing net greenhouse gas emissions. Initially, interest in this process was limited due to its operational complexity and the challenges associated with catalyst management. However, with the increase in environmental awareness and the need to reduce CO_2 emissions, dry reforming has become an area of active research (Navarro, 2007).

Therefore, in recent years, significant progress has been made in the development of catalysts that are more efficient and resistant to decommissioning caused by solid-phase carbon deposition (Wang, 2000). Catalysts based on noble metals, such as platinum and rhodium, are highly effective, but their high cost limits their use on a large scale. As a result, research has focused on nickel-based catalysts, which offer a good balance between cost and efficacy (Abdullah, 2017).

Technological innovations also include modifying catalytic supports to improve active metal dispersion and sintering resistance. Supports such as magnesium oxide (MgO), alumina (Al_2O_3) and titanium dioxide (TiO_2) have been extensively studied. In addition, promoting catalysts with other metals, such as cerium (Ce) or calcium (Ca), has been shown to improve catalyst stability and durability (Matus, 2012).

Recently, research has also explored the integration of dry reforming with other gas conversion processes, such as steam reforming and partial oxidation, to form hybrid processes that optimize syngas production and minimize CO_2 emissions (Murthy, 2002). These hybrid processes can improve overall energy efficiency and operational flexibility, making dry reforming a more competitive option for syngas production.

Despite progress, dry methane reforming continues to present several challenges. The main one is the management of carbon deposition in catalysts, which can lead to decommissioning and reduce process efficiency. In addition, the need to operate at very high temperatures comes with significant engineering challenges and energy costs.

To address these challenges, research focuses on new catalyst formulations and advanced reactor technologies, such as membrane reactors and microchannel reactors, which can improve heat and mass transfer and reduce plant size (Gallucci, 2008). In addition, the use of renewable energies to power the dry reforming process is an area of great interest, with the aim of making the process more environmentally sustainable.

Dry methane reforming has considerable application potential, especially in natural gas recovery and CO_2 management. The syngas produced can be used in a variety of industrial processes, including the synthesis of liquid fuels through Fischer-Tropsch, the production of methanol, and the synthesis of basic chemicals (De Smet, 2001).

The DRM process can be summarized in the following reaction:

$$CH_4 + CO_2 \rightarrow 2H_2 + 2CO \quad (3)$$

In this way, this process allows the use of two greenhouse gases as reactants to produce hydrogen and carbon monoxide. Therefore, dry methane reforming can help reduce net CO_2 emissions into the atmosphere and offers the possibility of converting exhaust gases and industrial waste into products.

6.3. PROBLEMS IN INDUSTRIAL APPLICATION

However, there are still challenges to overcome to make dry methane reforming more economically competitive and commercially attractive than other options. Therefore, making DRM a worthy competitor for steam reforming in the industrial sector entails several challenges to overcome related to the operating conditions of the reaction, in particular the high temperatures required for the reaction, as well as the management of by-products and the durability and regeneration of catalysts (Leung, 2007).

Dry reforming is a slow reaction that requires a large amount of energy (in the form of heat) to dissociate the highly stable molecules CO_2 (526 kJ mol−1) and CH_4 (435 kJ mol−1). It is also necessary to reach equilibrium and convert these molecules into synthesis gas with relatively short residence times, which makes the reaction an object of study for future industrial applications. In addition, at the same time as DRM, there are several secondary reactions that affect the balance of the reaction, among which the following three can be highlighted:

1. Water Gas Displacement Reverse Reaction (RWGS):

$$CO_2 + H_2 \rightarrow CO + H_2O \quad (4)$$

2. Methane decomposition:

$$CH_4 \rightarrow C\,(s) + 2H_2 \quad (5)$$

3. Boudouard's reaction:

$$2CO \rightarrow CO_2 + C\,(s) \quad (6)$$

In this way, the RWGS reaction increases the conversion of CO_2, producing a syngas with an H_2/CO ratio of less than 1. In addition, the other two reactions, which lead to the formation of solid carbon in the form of coke, cause the catalyst to disable the blocking of the catalyst's active sites (Wang, 2012).

Thus, the objective of this work is to optimize the H_2/CO ratio by studying nickel and nickel/cobalt catalysts and to implement innovative strategies for the removal of coke deposited during the reaction, in order to extend the useful life of these catalysts.

7. BIBLIOGRAPHIC REVIEW

7.1. CERAMIC HONEYCOMB VS CERAMIC OPEN FOAM FOR DMR

Before proceeding with the execution of the pilot project, it is essential to understand some aspects related to the decisions made with reference to the mode of operation, the catalysts used, and the support for them. In this sense, several articles extracted from the scientific literature published in recent years have been studied to justify the choices made.

First of all, a fundamental aspect to take into account when carrying out the work operation is the choice of a suitable support for the catalysts, as well as an appropriate active phase. Over time, various types of supports for metal catalysts have been studied. The most effective ones, in order to understand how to improve the efficiency of the DRM reaction, are open foam supports and monoliths (Ciambelli, 2009). The research therefore analyzed, for both structures, their resistance to possible mechanical stresses, the adhesion of the catalyst to them, and whether the operating conditions would change in each case.

For one, monoliths offer a textured geometric surface that can be advantageous in some applications, as shown in Figure 1. These monoliths have a high density of regular channels, which can be useful for uniform distribution of reagent flow and for maximizing contact between the catalyst and the reactants. However, the structure of monoliths also has some disadvantages, such as lower efficiency in maintaining a uniform temperature throughout the catalytic bed, especially in large reactors (Ciambelli, 2009). In addition, monolith preparation requires more complex procedures to ensure uniform adhesion of the catalytic layers and uniform distribution of the catalyst along the monolith channels.

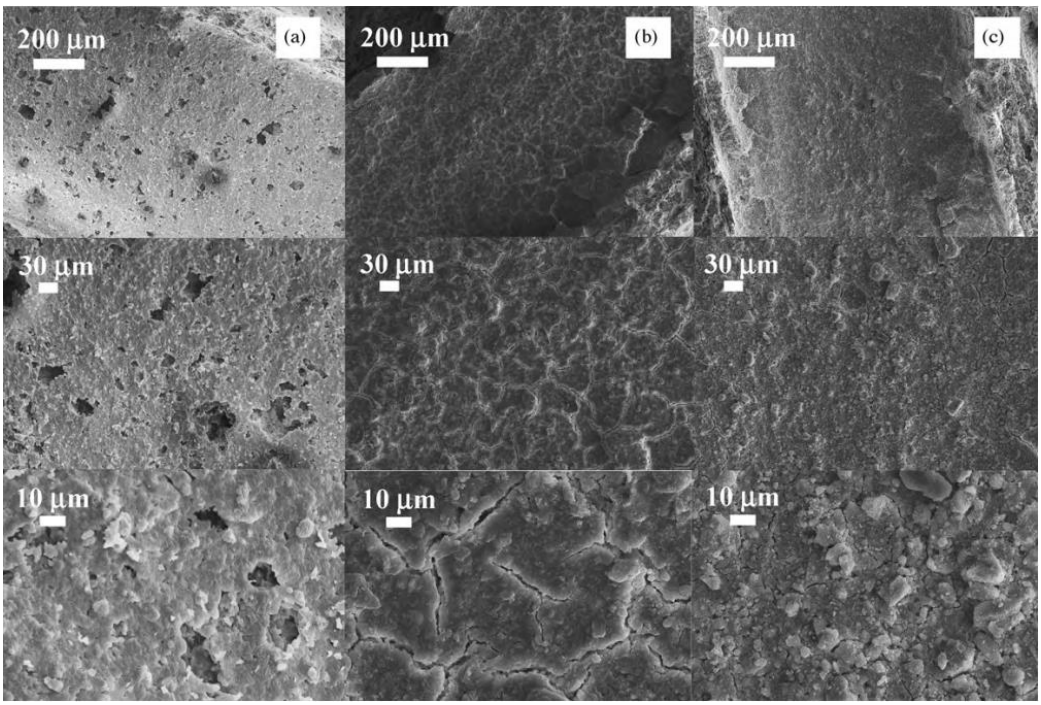

Figure 1.- SEM images of a cordierite monolith (a), a washed monolith (b) and a monolith after the deposition of Ni (c), at different magnifications.

On the other hand, in the field of catalysis, it has been shown that the use of ceramic foam structures offers significant advantages over traditional monoliths. As shown in Figure 2, open-cell foams are characterized by a highly interconnected porous structure, which provides a high specific surface area and uniform pore distribution, facilitating uniform anchoring of the catalyst (Ciambelli, 2009). This porous structure also promotes better diffusion of reactants and products within the catalyst, improving the efficiency of reforming reactions. In addition, the open nature of the foam cells allows for better heat exchange within the catalytic bed, which helps maintain a more uniform temperature throughout the reactor bed. The use of open-cell foams can also promote greater mechanical strength of the catalyst, reducing the risk of damage due to vibrations or thermal shocks during operation.

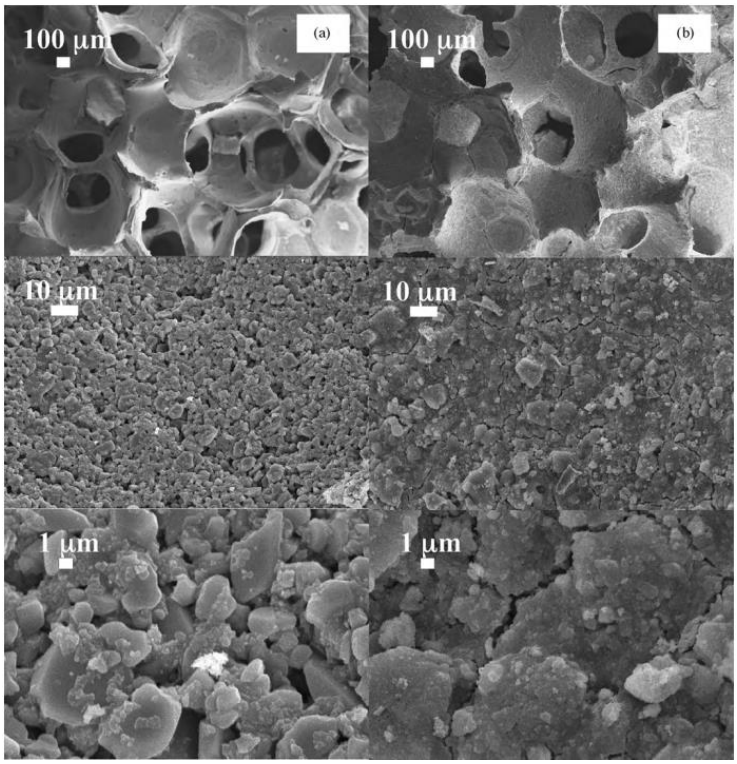

Figure 2.- SEM images of a calcined ceramic foam before (a) and after washing and deposition of Ni (b), at different magnifications.

Comparing the results, open-cell foam offers several advantages over honeycomb monoliths:

1. Maximum reduction at lower temperatures: Ceramic foam exhibits the greatest reduction of NiO at lower temperatures than honeycomb structure, indicating greater catalytic activity at lower temperatures. The maximum NiO reduction temperature for ceramic foam is 425 °C compared to 470 °C for the monolithic structure.

2. Maximum reduction intensity: Ceramic foam shows higher stability and less formation of unwanted by-products than monolith.

3. Reduced crystallite size: The foam is composed of a smaller crystallite size, which provides a larger active surface area for the catalyst and better exposure of the activated nickel atoms.

4. Catalytic Layer Adhesion: Foams, when subjected to proper heat treatment, exhibit better adhesion of the wash layer, contributing to greater catalyst stability.

5. Resistance to stress tests: Foams are more resistant to stress tests, such as ultrasonic vibrations and thermal shocks.

6. Uniformity of catalyst distribution: Foams can offer a more uniform distribution of the catalyst throughout the substrate, due to their porous structure and greater flexibility in the process of incorporating the catalytic layer.

In addition to these advantages, the geometric characteristics of the foams play a crucial role in their catalytic performance. Table 1 summarizes the key properties of OCF structures with different pore densities (20, 30, and 40 ppi), highlighting the relationship between pore size, catalyst deposition, and surface area.

Geometric Property	OCF 20 ppi	OCF 30 ppi	OCF 40 ppi
Average pore diameter (mm)	1.92	1.40	1.08
Average strut thickness (mm)	0.51	0.41	0.33
Relative density (ρr)	0.11	0.13	0.14
Total porosity (ε)	0.89	0.87	0.86
Geometric surface area (GSA, m^2/m^3)	669	967	1273
Catalyst loading (mg/cm^2)	22.2	15.2	12.0
Catalytic layer thickness (μm)	25–40	15–30	5–20

Table 1.- Geometrical characteristics of the investigated open cell foam (OCF) structures.

From this data, it emerges that increasing the pore density leads to a reduction in pore size and strut thickness, while simultaneously increasing the available geometric surface area (GSA). This has direct implications for catalytic efficiency, as a higher GSA enables a thinner catalytic layer, improving mass and heat transfer properties. The porosity remains relatively high across all configurations, ensuring efficient gas diffusion.

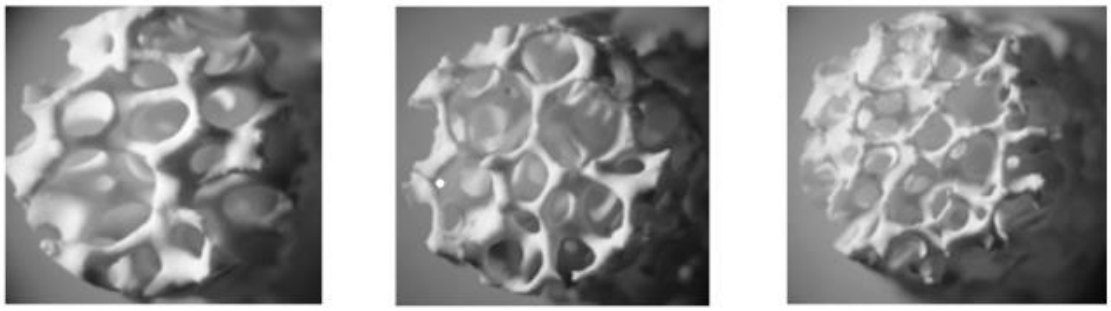

Figure 3.- Microscope image of the different structures of the OCFs.

In conclusion, research conducted on a series of nickel catalysts structured with monolithic foam and ceramic in the ATR process has determined that open-cell foam substrates perform

better than monoliths. A preparation procedure was developed that highlighted the key parameters influencing the quality of the catalytic layer adhesion, substrate pretreatment, and drying speed. Catalytic activity tests showed that in the GHSV range studied, foam-forming catalysts allowed for higher activity than honeycomb catalysts, as well as a lower average temperature along the catalytic bed and a more uniform temperature profile. The increased geometric surface area in high-ppi foams results in a thinner, well-distributed catalytic layer, reducing mass transfer limitations and ensuring a more stable and efficient reaction. The improved heat exchange capabilities of OCFs also help prevent hot spots, which can cause catalyst sintering and deactivation over time.

Therefore, although both structures offer specific advantages, the use of open-cell foam may be preferable in many applications due to its highly porous structure, which promotes better adhesion of the catalytic layer, uniform distribution of heat and reactants, and greater mechanical strength (Ciambelli, 2009). The data from Table 1 further emphasize that OCFs with 40 ppi exhibit the best performance in terms of catalytic efficiency, making them the ideal choice for industrial-scale Dry Reforming of Methane applications aimed at syngas and hydrogen production (Specchia, 2018).

7.2. DRM WITH NICKEL BASE CATALYSTS

7.2.1. Characteristics of Nickel

Research on active, stable and selective catalysts for dry methane reforming is dominated by nickel-based catalysts.

Nickel stands out as an excellent catalyst for the DRM reaction for a number of key reasons. Firstly, it has remarkable catalytic activity, facilitating the breaking of C-H and C-O bonds in reactants, i.e. methane and carbon dioxide, and promoting the formation of desired products, such as carbon monoxide and hydrogen. In addition, nickel enjoys good thermal stability, which means that it can withstand the high temperatures required for the DRM reaction without undergoing significant sintering or loss of catalytic activity (Zhu, 2010).

An additional advantage of nickel is its low cost: it is relatively cheap compared to other precious metals such as platinum and palladium, which could be used as alternative catalysts. This economic aspect is further amplified by its abundance in the Earth's crust, making it readily available for large-scale catalyst production (Rustrup-Nielsen, 2002).

Finally, nickel shows good tolerance to sulfur. Even in the presence of trace amounts of sulfur in the reactants, which is common in natural gas and biogas, nickel retains its catalytic activity better than many other metals. These combined characteristics make nickel an ideal choice for use as a catalyst in the DRM reaction (Wang, 1998).

However, combining nickel with other elements can lead to better DRM efficiency, resulting in lower coke deposition and a higher H_2/CO ratio. In reference to this, in this work several combinations of catalysts have been studied to understand which one satisfies and improves the conditions mentioned above. Therefore, nickel-based catalysts were prepared by the coprecipitation method and calcined at 800 °C with the aim of obtaining NiX_2O_4 structures with X = Cr, Mn and Co. Subsequently, the catalysts were tested for the DRM reaction without any hydrogen pre-treatment (Rouibah, 2017).

7.2.2. Nickel – Manganese

The nickel-manganese (Ni-Mn)-based catalyst showed a crystal structure dominated by the spinel phase of $NiMn_2O_4$, however, the presence of minor phases such as Mn_2O_3 and NiO indicated a complex composition of the catalyst. As shown in Figure 4, the reducibility of the catalyst was evidenced by the reduction temperature of manganese oxide Mn_2O_3 and spinel $NiMn_2O_4$ observed at 390 °C, indicating a potential for good catalytic activity.

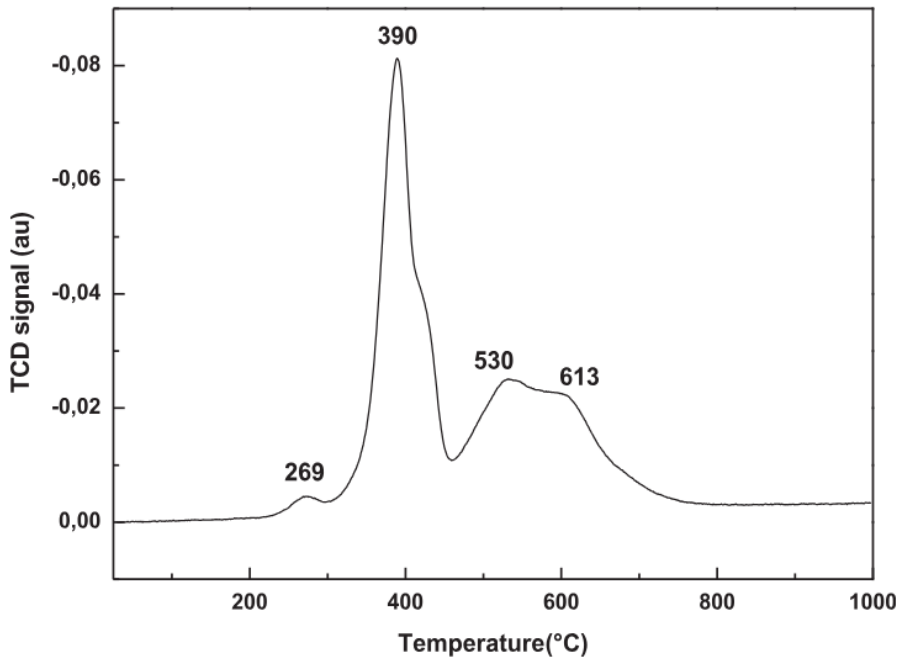

Figure 4.- H2-TPR profile of the Ni-Mn catalyst prepared by coprecipitation.

Scanning electron microscopy (SEM) revealed local variations in contrast and different crystal sizes, suggesting a mixed catalytic structure consistent with the results of X-ray diffraction (XRD) and Raman spectroscopy. However, the analysis of the catalytic yield showed that the Ni-Mn catalyst underperformed compared to the other two catalysts, with higher coke production and lower selectivity towards the syngas, suggesting lower efficiency in the DRM process.

7.2.3. Nickel - Cobalt

The nickel-cobalt (Ni-Co) catalyst showed a predominant phase of Co_3O_4 with a spinel structure, while the predicted phase of $NiCo_2O_4$ was not detected. Raman spectroscopy showed peaks consistent with the presence of Co_3O_4, indicating a normal structure of the $Co(Co)_2O_4$ spinel. As shown in Figure 5, catalyst reduction occurs in two stages, with Co_3O_4 reduced to Co0 at 405°C and Ni^{2+} reduced to Ni0 at higher temperatures, revealing a distinctive reduction sequence.

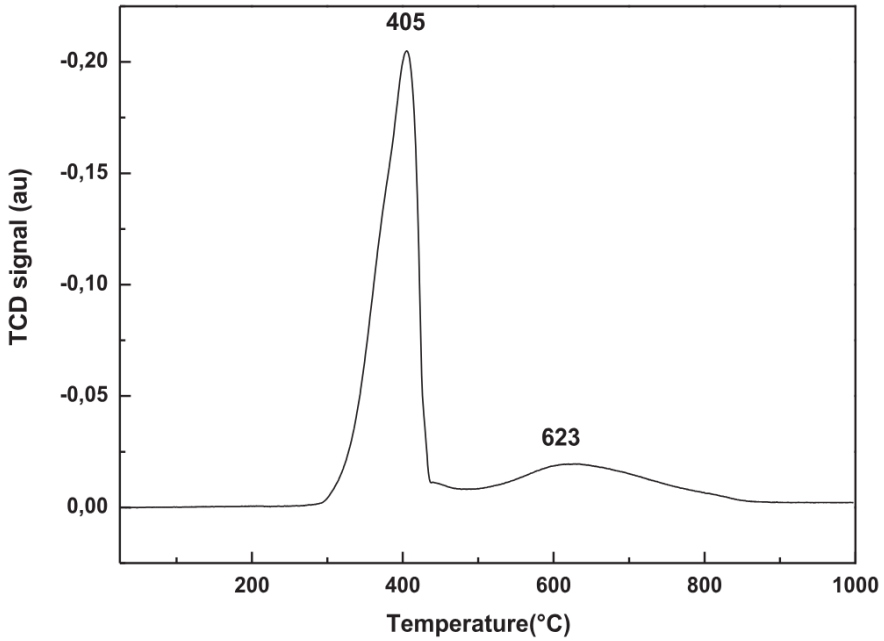

Figure 5.- H2-TPR profile of the Ni-Co catalyst prepared by coprecipitation.

However, despite the low surface area, the Ni-Co catalyst showed good catalytic activity in the DRM process, with high CH_4 and CO_2 conversions. In addition, its high selectivity towards hydrogen and lower coke formation indicate good process efficiency.

7.2.4. Nickel - Chromium

The nickel-chromium catalyst (Ni-Cr) had a complex composition with the presence of different phases such as $NiCr_2O_4$, Cr_2O_3 and NiO. Figure 6 shows that catalyst reduction occurred in multiple stages, revealing complex reduction dynamics.

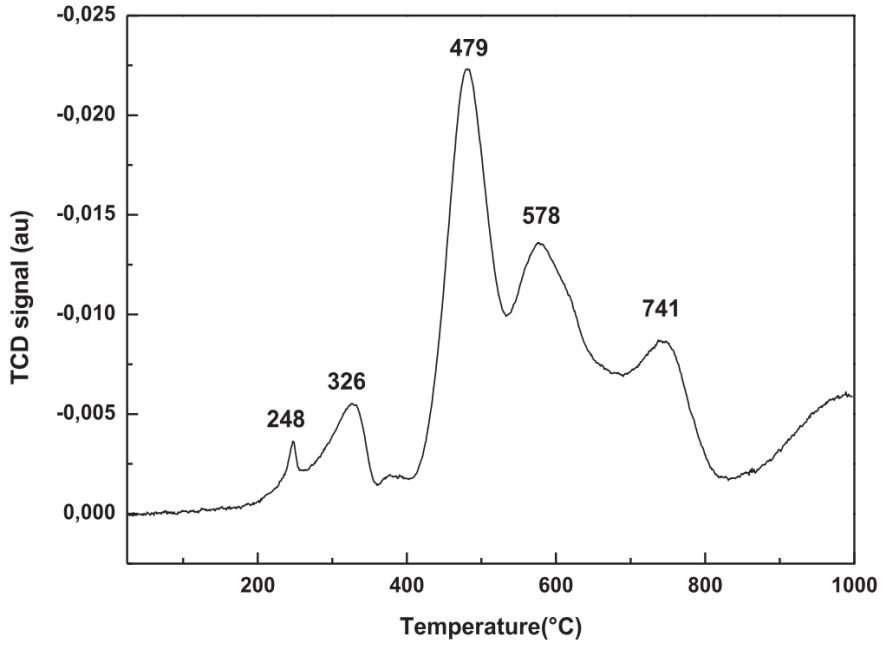

Figure 6.- H2-TPR profile of the Ni-Cr catalyst prepared by coprecipitation.

However, the Ni-Cr catalyst showed the highest catalytic activity among the three catalysts studied, with higher thermodynamic conversions for methane and H_2/CO values close to unity. This catalyst also showed minimal coke formation, indicating greater stability in the process. The significant presence of chromium oxide Cr_2O_3 (61%) has been identified as an important factor contributing to the stabilization of the active nickel sites on the catalyst surface.

In summary, the data indicated that the three catalysts exhibited different surface properties, with Mn mainly on the surface of the Ni-Mn system, in contrast to the Ni-Co system, and the same composition in the mass and surface of the Ni-Cr catalyst.

7.2.5. Comparison of catalytic activity

DRM tests were performed at temperatures between 700 and 800 °C, with a CH_4/CO_2 molar ratio of 1. The catalysts showed high activity with high selectivity towards the syngas. In all cases, the catalytic activity increased with the reaction temperature, with the best performance being observed at 800 °C. The results reveal the essential role of the promoter element (Cr, Mn and Co) and the structures of spinel (NiX_2O_4).

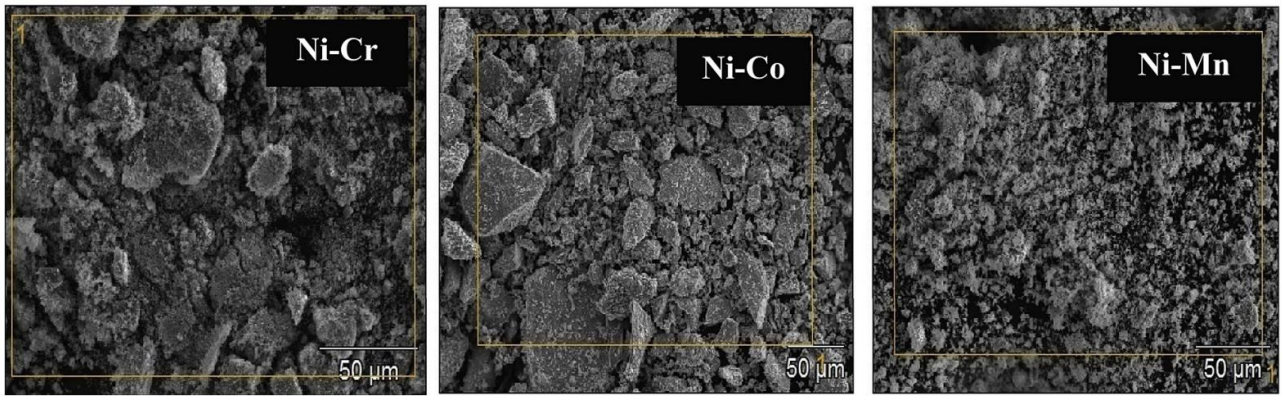

Figure 7.- SEM images of Ni-Cr, Ni-Co and Ni-Mn catalysts.

Among the three catalysts studied, the Ni-Cr catalyst showed the highest catalytic activity, with higher CH_4 and CO_2 conversion, H_2/CO molar ratios greater than 1 and lower coke deposition compared to the other catalysts. H_2/CO values, particularly at 700 °C, indicate that the Boudouard reaction also occurred at 750 and 800 °C. On the other hand, a low amount of deposited coke (4% of the converted CH_4) and a very high selectivity towards H_2 (> 99%), due to the low contribution of methane cracking reactions and RWGS.

In conclusion, the Ni-Cr catalyst showed excellent catalytic behavior in the DRM reaction. In contrast, the Ni-Mn sample showed a very different catalytic behavior than Ni-Cr, mainly due to the low surface nickel content detected by the XPS analysis. As a result, the catalyst containing Mn produced a significantly higher amount of coke, leading to a fairly low selectivity towards H_2 of between 61% and 80%. Finally, the Ni-Co catalyst has also shown good activity in the DRM reaction. This activity could be attributed to the high reducibility of the sample in the reaction environment. In addition, the H_2 selectivity of this catalyst was higher than that of Ni-Mn at the three temperatures tested, which highlights the role of spinel structures, as shown in Table 2, and of Co active sites in the DRM reaction (Rouibah, 2017).

Catalyst	T°(C)	X (%) CH_4	X (%) CO_2	C $(\%)_{produced}$	H_2/CO (±0.05)	H_2sel (%) ($H_2/(H_2 + H_2O)$)
Ni-Cr	800	94 (94[a])	91 (97[a])	4	1.2 (0.97[a])	99.6
	750	88 (86[a])	86 (94[a])	4	1.2 (0.95[a])	99.1
	700	84 (81[a])	81(88[a])	13	1.3 (0.92[a])	95.3
Ni-Mn	800	92	94	37	0.96	80.4
	750	86	91	62	1.01	66.1
	700	74	84	64	0.95	61.2
Ni-Co	800	83	87	13	0.96	91.1
	750	52	67	5	0.77	83.1
	700	28	42	<2	0.58	74.0

[a] Theoretical equilibrium values.

Table 2.- Reaction parameters in the dry methane reforming of the three catalysts studied.

Therefore, the study of catalysts in DRM allows us to conclude that:

1. All three catalysts studied were highly active in DRM despite their low specific area. The catalytic activity varied according to the order Ni-Cr>Ni-Co>Ni-Mn, which shows the role of structural properties.

2, The best results were obtained with the Ni-Cr catalyst. The catalytic behavior of this catalyst could be related to its homogeneity, reducibility, porous nature, crystal size and the presence of chromium oxide Cr_2O_3 (61%) that could contribute to the stabilization of the active sites of nickel on the surface.

3. The most important coke deposition was observed in the Mn-based catalyst. This could be related to the high Mn content on the surface and the low dispersion of Ni.

These results, and in particular for Ni-Cr, show that spinel structures can be interesting precursors of DRM-active catalysts. These results pave the way for future research that will allow us to better understand the actual active phase and, for example, the role of Cr_2O_3 (Rouibah, 2017).

7.2.6. Disadvantages of using chromium

However, recent studies have led to new insights into the above findings, as during the preparation of the nickel-chromium catalyst by calcination at elevated temperatures (such as 800 °C), oxidation of trivalent chromium (Cr^{3+}) present in chromium compounds used for catalyst synthesis could occur. Subsequently, during the DRM reaction, the chromium present in the catalyst may be subject to changes in the oxidation state due to the high temperatures and chemical reactions involved in the process. Therefore, if chromium is exposed to conditions conducive to oxidation, the formation of hexavalent chromium (Cr^{6+}) can occur (Goulas, 2017).

Hexavalent chromium is known to be carcinogenic to humans and has been associated with numerous health problems, including lung cancer, skin cancer, and other diseases (Gibb, 2000). However, it is important to note that the formation of hexavalent chromium also depends on the specific conditions of the reaction, such as the presence of oxygen, temperature, and pressure (Ukhurebor, 2021). For this reason, although its performance is not as high, nickel-cobalt catalyst is preferable to nickel-chromium catalyst for the DRM reaction.

7.3. DRM WITH COBALT BASE CATALYSTS

7.3.1. Characteristics of Cobalt

To further reinforce the use of cobalt, this 2024 study by the Royal Society explains and describes the effectiveness of this catalyst by making it work synergistically with other metals (noble and non-noble) including nickel. Cobalt-based catalysts have undergone rapid development in recent years and have gradually demonstrated their particular superiority due to their particular chemical and physical characteristics, especially the search for cobalt-based bimetallic catalysts, which has become a long-term challenge.

Following in the footsteps of previous work, in cobalt-based catalysts, several transition metals, such as Pt, Ru, Rh and Ni, have been added as secondary metals, and some significant advances have been made in this field. This research summarizes the application of cobalt-based catalysts in the DRM reaction and its oxygen storage mechanisms, active metal dispersion, metal-support interaction, modification of surface chemical properties, and surface basicity (Sun, 2024).

7.3.2. Cobalt - Platinum

The addition of noble metals to cobalt catalysts can improve the binding strength of oxygen species, greatly increasing catalytic activity and strength. The intrinsic behavior of the noble metals and the favored reducibility contribute to the excellent activity of these bimetallic catalysts compared to monometallic samples.

In particular, Pt doping of these catalysts can enhance the reducibility of cobalt, thereby increasing catalyst activity. The H_2-TPR results showed that the Co supported in TiO_2-Al_2O_3 modified with different Pt contents could be reduced more easily than the monometallic catalyst Co/TiO_2-Al_2O_3. The decrease in the Co reduction temperature is mainly due to the hydrogen spillover effect. The catalyst with 5% Co wtw and 0.5% Pt wtw demonstrated the best stability for the DRM reaction.

Compared to the monometallic catalyst, the formation of Pt-Co alloys played the role of the main active structure, even though both the separated Co particles and the bimetallic alloy coexisted in the catalysts. The presence of Pt significantly improved the reducibility of cobalt oxides, demonstrating a strong interaction between Pt and Co. In addition, DFT calculations and kinetic studies showed that the addition of Pt reduced the activation barrier of the C-H bond, generating fewer coke deposits in the spent catalyst (Sun, 2024).

7.3.3. Cobalt - Ruthenium

Of all the noble metals, Ru is considered a possible alternative to Pt due to its relatively low cost. In addition to improving catalytic activity, the incorporation of Ru into Co-based catalysts makes them more suitable for industrial application in the DRM process. The effect of Ru on the catalytic performance of the Co/SBA-15 system for the DRM reaction with different Ru charges was investigated. The catalyst with 5% Co wtw and 0.1% Ru wt% showed optimal catalytic performance. It was observed that Ru particles generally occupied the outside of the pores, while Co particles occupied both the inside and outside of the pores.

The doping of Ru decreased the reduction temperature of the catalysts, with an increase in the amount of Ru displacing the reduction to lower temperatures, due to the indirect effect of hydrogen from the cobalt oxide species that reduce the promoter of Ru. Catalytic performance improved significantly as Ru loading increased, but there was no significant improvement when Ru loading exceeded 0.14% by weight. In addition, the catalytic performance of Co-Ru/SiO_2 was found to be much better than that of the monometallic catalyst Co, confirming that an adequate concentration of Ru on the surface of the catalyst improves oxidation resistance and resistance to coke formation (Sun, 2024).

7.3.4. Cobalt - Rhodium

In addition to the noble metals Pt and Ru, Rh can also adjust the electronic structure to improve catalytic performance. The bimetallic catalyst Rh-Co has been confirmed to possess excellent catalytic activity for the DRM reaction. Comparison of the promotional effect of different metals (Ni, Rh and Ru) in a sample based on Co/Al_2O_3 showed that the catalyst promoted by Rh had optimal catalytic activity at different reaction temperatures. This performance improvement is related to the formation of nanocrystalline spinel from cobalt aluminate with good redox properties. In addition, CO_2 dissociation was more likely in the Rh-promoted samples in the presence of CH_4, and the modified catalyst showed greater activity in the DRM reaction than in the unmodified ones.

In summary, for non-noble metal catalysts, the addition of noble metals greatly improves catalytic performance. However, the high cost makes it difficult to use these catalysts on a large scale, unless the noble metal load is extremely low (Sun, 2024).

7.3.5. Cobalt - Nickel

The addition of Ni can increase the number of active sites for the decomposition of CH_4 and CO_2. Co-Ni-based catalysts have better redox properties than any non-noble monometallic catalyst. Compared to Ni-based monometallic catalysts, the addition of a small amount of Co can effectively improve catalytic performance, mainly due to Co's strong affinity for active oxygen. However, Co can oxidize quickly, causing the catalyst to deactivate. In subsequent studies, it has been observed that CO_2 partially oxidizes Co to CoO and is then reduced to Co^0 when it comes into contact with carbon species generated by the decomposition of CH_4. Therefore, the presence of cobalt can effectively inhibit carbon deposition and improve catalyst stability, due to its ability to adsorb CO_2 and the strong interaction of the Co-O bond.

The Ni/Co ratio has a significant impact on the physical properties of the catalyst, influencing the efficiency of mass transfer. Promoting Ni-based catalysts with a small amount of Co is sufficient to improve catalyst stability, but too much Co can reduce catalytic activity. Studies have shown that a Ni/Co molar ratio of 9:1 provides excellent stability in the DRM reaction, mainly due to the reduction of carbon deposition. Similar results were observed with lower Co/Ni ratios, showing a good balance between oxidation and reduction, where Ni dissociates CH_4 and Co promotes the oxidation of CHx species.

On the other hand, catalysts with high Ni and Co loads (50%) showed the best catalytic performance, while high Co loads led to poor catalytic stability and the accumulation of carbon

deposits at elevated temperatures. Catalysts with a higher concentration of cobalt were more active and selective towards H_2, but also generated a large amount of coke, attributed to increased Co activity in CH_4 decay.

In bimetallic Ni-Co samples, the addition of Co reduced the Ni particle size, improved the stability of the catalyst, and facilitated the formation of a Ni-Co alloy with a strong interaction between the two metals, preventing sintering of the active metal. The Ni-Co alloy, with a higher electron density in Ni, prevented the complete decay of CH_4 in the coke deposits. In addition, the addition of Co contributed to CO_2 adsorption and activation, which led to increased CO_2 conversion and a significant improvement in catalyst stability, preventing undesirable side reactions (Sun, 2024).

7.3.6. Comparison of catalytic species

In this way, the results showed that several cobalt-based catalysts have excellent catalytic properties, such as high activity, high stability, and excellent resistance to coke formation at high reaction temperatures in the DRM reaction (Wang, 2022).

Despite these successes, there are still several issues that need to be addressed in the development of cobalt-based catalysts for the DRM reaction. The future direction of research should focus more on the mechanism and theoretical study of the reaction and on the research and development of new catalysts. For example, the development of supports with porous structures to improve the stability of DRM catalysts by firmly anchoring the active metals, so that a method of dispersing the active metals in atomic form can be developed to increase the active sites of the catalyst and enhance its activity (Sun, 2024). Similarly, the low-temperature DRM reaction should also be studied to achieve additional benefits in terms of energy savings and environmental protection (Chen, 2023).

8. EXPERIMENTAL PART

8.1. CATALYTIC SYNTHESIS

The catalyst was synthesized via the solution-fired synthesis (SCS) pathway. Following this methodology, solutions with adjusted concentrations of $Ni(NO_3)_2 \cdot 6H_2O$, $Al(NO_3)_3 \cdot 9H_2O$ and $Co(NO_3)_2 \cdot 6H_2O$, together with glycine, were prepared. In all solutions, the nitrate concentration was fixed at 4 mol $^{L-1}$. Similarly, to obtain the monometallic catalyst Ni, the molar Ni/Al ratio of the solution was set at 0.5; while to obtain the bimetallic Ni-Co catalyst, the molar ratio (Ni+Co)/Al was set at 0.5 and the molar Ni/Co ratio at 1.

In this synthesis method, glycine ($C_2H_5NO_2$) was used as fuel oxidized by nitrates in solution. The use of glycine in catalyst synthesis through the SCS method offers several key advantages. Glycine acts as a fuel that reacts with nitrates, promoting vigorous combustion that generates enough heat to form metal oxides. This process makes it possible to obtain catalysts with high purity, chemical homogeneity and good particle size distributions. In addition, the method is simple, effective, and environmentally friendly (Carbos, 2018). The amount of glycine to be added to each solution was calculated as a stoichiometric point, according to the following reactions:

$$Ni(NO_3)_2 + \frac{10}{9} C_2H_5NO_2 \rightarrow NiO + \frac{20}{9} CO_2 + \frac{25}{9} H_2O + \frac{14}{9} N_2 \quad (7)$$

$$Al(NO_3)_2 + \frac{5}{3} C_2H_5NO_2 \rightarrow \frac{1}{2} Al_2O_3 + \frac{10}{3} CO_2 + \frac{25}{6} H_2O + \frac{7}{3} N_2 \quad (8)$$

$$Co(NO_3)_2 + \frac{28}{27} C_2H_5NO_2 \rightarrow \frac{1}{3} Co_3O_4 + \frac{56}{27} CO_2 + \frac{70}{27} H_2O + \frac{17}{11} N_2 \quad (9)$$

Once the solutions were prepared, the next step was to put them in contact with the previously selected support. In this case, α-Al_2O_3 open-cell ceramic foams were used, with dimensions of 10 mm in length and 8 mm in diameter. Each foam block was immersed in one of the two solutions for 5 minutes, after which the excess was removed with compressed air. The impregnated foams were then placed in a 300°C furnace for 30 minutes to start the combustion process. This impregnation and combustion process was repeated a total of 5 times, until a total active phase load of approximately 10-11% of the total weight of the foam was achieved (Figure 7). Finally, the foams were placed in a furnace at 850 °C for 4 hours, in order to form the $NiAl_2O_2$ and $CoAl_2O_4$ spinels through the solid-state reaction of the NiO, Al_2O_3 and Co_3O_4 oxides formed during the combustion cycles.

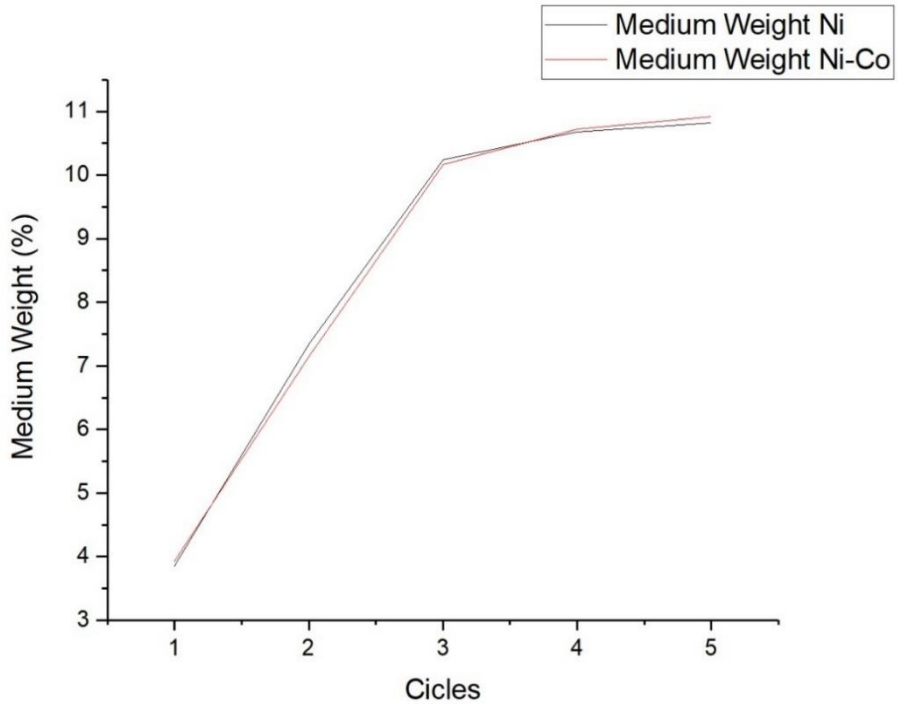

Figure 8.- Evolution of the metallic charge of the foams with the number of SCS cycles.

The graph in Figure 8 illustrates the average percentage increase in weight of nickel- and nickel-cobalt impregnated catalysts. As can be seen after the third cycle, the percentage by weight increases by a smaller amount, this is because the deposited catalytic layer absorbs less solution than the surface of the clean ceramic foam, which reduces the mass of the deposited catalytic layer in subsequent cycles.

The use of SCS in catalyst synthesis offers several significant advantages. This method allows the production of materials with high chemical homogeneity and nanostructured morphology. The rapid reaction and high-temperature gradients promote the formation of unique microstructures that are not achievable with conventional methods.

Furthermore, SCS is adaptable to different structured substrates, such as ceramic and metallic monoliths, making it particularly useful for the preparation of supported catalysts. Due to its high efficiency, this method has also been successfully employed in the production of catalytic burners used for natural gas combustion in domestic applications. Compared to conventional burners, catalyzed ones present a lower environmental impact, thanks to better combustion process stabilization and reduced CO and NOx emissions.

Despite the numerous advantages, SCS presents some challenges, such as the potential formation of NOx during synthesis, due to the thermal decomposition of nitrates before the main reaction ignition. However, this issue can be mitigated using selective abatement systems.

Overall, solution combustion synthesis remains a promising and effective technique for the production of advanced catalysts, offering a balance of simplicity, cost-effectiveness, and high performance (Specchia, 2010).

8.2. CHARACTERIZATION TECHNIQUES

8.2.1. X-ray diffraction (XRD)

The crystallography of catalysts is a crucial aspect of understanding their properties and functioning. To accurately assess the average crystal size and identify the crystal phases present in samples, the X-ray diffraction (XRD) technique is indispensable. This methodology not only allows for detailed structural characterization of catalytic materials, but also provides fundamental information about their atomic organization and the size of the crystal domains. Through diffraction pattern analysis, it is possible to infer the internal arrangement of the atoms and any imperfections present in the crystal structure, offering a deep understanding that is essential to optimize catalyst performance.

X-ray diffraction is a structural analysis technique that allows the main crystallography of samples to be determined and their subsequent study by estimating the size of the phase crystals present in them. Bragg's law is a fundamental principle used in X-ray diffraction analysis. This law provides a relationship between the angle of incidence of radiation, the wavelength, and the distance between the lattice planes in a crystal. Therefore, Bragg's law is expressed as:

$$n\lambda = 2dsen\,(\theta) \tag{10}$$

Where:

d is the distance between the crystalline planes

θ is the angle of incidence of radiation

λ is the wavelength of the radiation

n is an integer that represents the order of the diffraction peak. Bragg's law is fundamental for the interpretation of X-ray diffraction data, since it allows determining the interplanar distance within a crystal by knowing the angle of incidence of the radiation and the wavelength used (Bragg, 1913).

On the other hand, the Scherrer equation is also used to estimate the size of crystals of a given phase by their diffraction peaks. This equation is particularly useful when you want to obtain information about the average size of crystals without the need for a detailed analysis of the crystal structure. The Scherrer equation is expressed as:

$$\tau = \frac{K\lambda}{\beta\cos\,(\theta)} \tag{11}$$

τ is the average size of the crystals (in nanometers)

K is a form factor (usually between 0.9 and 1, depending on the shape of the crystal),

λ is the wavelength of the radiation used in diffraction

β is the width at half-height (FWHM) of the diffraction peak (in radians)

θ is the diffraction angle

The Scherrer equation is derived from the Debye-Scherrer law, which deals with the diffraction of polycrystalline crystals, i.e., samples containing many small, randomly oriented crystals. The

equation provides an estimate of the average size of crystals in a sample based on width at half the height of the diffraction peak (Patterson, 1939). It is important to note that the Scherrer equation only provides a rough estimate of the size of the crystals and may be influenced by several experimental and theoretical factors. However, it remains a useful tool for obtaining qualitative information about crystal size in polycrystalline samples.

The experimental protocol of the analysis was carried out at the SGIker General Research Services of the University of the Basque Country UPV/EHU. The analyses were performed on a PANalytical X'Pert PRO diffractometer equipped with a monochromator tuned for Cu K_α radiation (λ = 1.5406 Å) and a Ni filter. Diffractograms were taken between positions 2θ = 5-80°.

8.2.2. Programmed Temperature Reduction with Hydrogen (H2-TPR)

Programmed temperature reduction (TPR) is an analytical technique used primarily to characterize catalysts. This technique provides detailed information on the reactivity of catalysts under reducing conditions. In a TPR test, a solid catalyst is exposed to a reducing gas, usually hydrogen or carbon monoxide, while the temperature is gradually increased in a programmed manner. During this process, the reactive functional groups present on the surface of the catalyst react with the reducing gas, causing the reduction of the compounds present. These reduction reactions are usually exothermic and therefore release heat.

In programmed hydrogen (H_2-TPR) temperature reduction, a reducible catalyst or catalyst precursor is exposed to a mixture of 5% H_2 in argon, while the temperature is increased in a controlled manner. During the experiment, the concentration of hydrogen in the reactor outlet stream is continuously measured through a TCD (thermal conductivity detector). The experiment makes it possible to determine the total amount of hydrogen consumed in the reduction of the material studied, as well as the temperature at which this reduction process is carried out. From these results it is also possible to calculate the degree of reduction of the sample and, consequently, the mean oxidative state of the solid before its reduction (Chin, 1993).

TPR experiments with H_2 were carried out on a Micrometrics Autochem II device. For each analysis, 0.1 g of sample was used, which was placed in a U-shaped quartz reactor, supported by quartz wool. The analyses were carried out following a temperature ramp of 10 °C $^{min-1}$ at a temperature of 950 °C. A cold trap was used at the exit of the reactor to prevent the formed water from reaching the TCD and altering the conductivity measurements. The trap was kept at a low temperature (< -10 °C) by means of an isopropanol paste cooled with liquid nitrogen to the melting point (Ertl, 2008).

8.3. STUDY OF CATALYTIC ACTIVITY

The study of the catalytic activity of the synthesized materials was carried out in a fixed-bed reactor of the PID Eng&Tech brand. This device consists of a quartz tubular reactor with a diameter of 9 mm that operates at atmospheric pressure. To increase the temperature of the reactor, it is heated by means of a cylindrical furnace with an electric heating element. The

temperature is measured by means of a K-type multipoint thermocouple inserted into the catalytic bed and controlled by a computer program.

In addition, the reactor has several gas supply lines that are controlled by mass flow regulators. The gases exiting the reactor are analyzed using an Agilent 990 microGC chromatograph, which consists of two channels, each equipped with a thermal conductivity detector (TCD). Channel A consists of a 10 m molecular sieve column with a pore size of 5 Å and a 3 m PBQ pre-column for measuring permanent gases such as H_2, N_2, O_2, and CO. Channel B contains a 10 m PPQ column for measuring CH_4 and CO_2. In addition, before reaching the chromatograph, the outgoing gases pass through a Peltier cooler to remove the water generated during the reaction, thus avoiding interference during chromatographic analysis.

The catalytic activity of all catalysts was studied following the same reaction process. Prior to each reaction assay, catalytic precursors were reduced in situ with a 5% H_2 flux in nitrogen at 850 °C, for 2 hours. Reaction tests were performed at a constant temperature of 650 °C, with a total flow rate of 800 cm^3 min^{-1} of a gaseous mixture of 10%CH_4/10%CO_2/80%N_2 for 72 hours. Therefore, the approximate space velocity was 96000 $^{h-1}$.

Figure 9.- Photograph of the fixed-bed reactor used in this study, located at the Department of Chemical Engineering of UPV/EHU.

9. RESULTS

9.1. CHARACTERIZATION OF CATALYTIC PRECURSORS

9.1.1. Properties of ceramic foam backings

Analysis of the structural properties of the ceramic foam supports by X-ray diffraction revealed a multiphase composition, including alpha-Al_2O_3, mullite, cristobalite, and cordierite in the non-impregnated foam. Integrating these ceramic materials into nickel and nickel-cobalt catalyst supports offers numerous benefits that can αimprove catalyst performance and durability.

Therefore, alpha-Al_2O_3, known for its hardness and thermal stability, provides a robust and wear-resistant structure, which is essential for effective catalyst dispersion and maintenance of long-term efficiency. Mulite, chosen for its mechanical and thermal resistance, contributes to the insulation of the catalyst due to its low thermal conductivity. Similarly, cristobalite offers thermal resistance, although its high thermal expansion is balanced by integration with other ceramic materials, improving resistance to thermal shock (Saruhan, 1996). One of the key aspects is the presence of cordierite, known for its very low thermal expansion and resistance to thermal shock. These characteristics are critical to ensuring the overall stability of the substrate during rapid temperature changes, reducing the risk of cracks and fractures. The combined effect of alpha-Al_2O_3, mullite, cristobalite, and cordierite results in a ceramic support structure that offers unprecedented thermal and mechanical stability.

In addition, the integration of these ceramic materials into catalyst carriers offers numerous operational advantages. The optimized specific surface of the supports allows an effective dispersion of the active catalyst, improving the efficiency of chemical reactions. Resistance to wear, chemical corrosion, and thermal fluctuations ensures stable and long-lasting performance, reducing the frequency of replacements and increasing the overall efficiency of catalytic processes.

Finally, the use of relatively inexpensive ceramic materials, such as alpha-Al_2O_3 and cordierite, contributes to the reduction of the overall costs of the catalyst, without compromising its performance (Saruhan, 1996). This integrated approach to optimizing ceramic supports for nickel and nickel-cobalt catalysts represents a breakthrough in catalytic materials engineering, promising a positive impact on a wide range of industrial applications (Taylor, 2016).

9.1.2. X-Ray Diffraction (XRD)

Subsequently, the X-ray diffraction results of the analyzed samples are studied, i.e. the precursors of Ni and Ni-Co and the metal catalysts of Ni and Ni-Co.

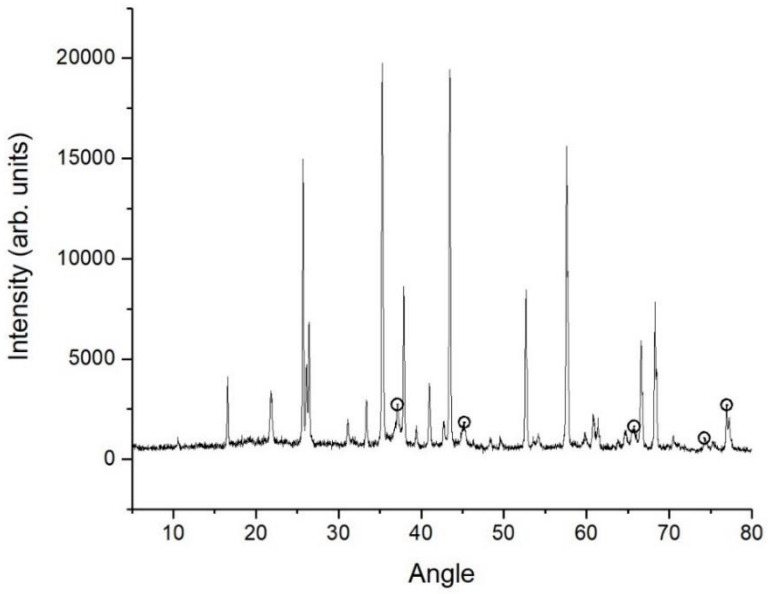

Figure 10. - X-ray diffractogram of the Ni aluminate precursor.

As shown in Figure 10, several highlighted diffraction peaks indicate the presence of a spinel phase, associated with the presence of nickel aluminate. Therefore, from these signals it is possible to estimate the size of the crystals through the Scherrer equation. Therefore, the size of the spinel crystals in the monometallic precursor was 15 nm.

The same procedure was performed with the bimetallic precursor Ni-Co with the results shown in the figure below.

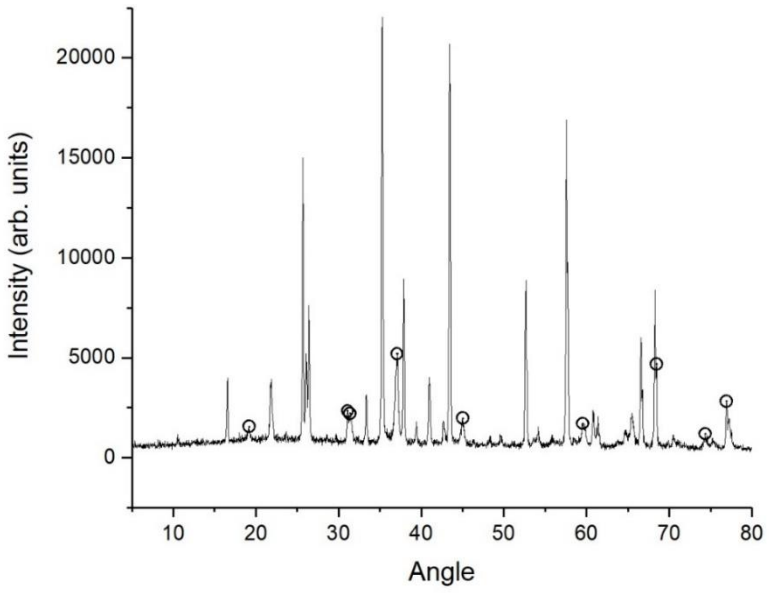

Figure 11.- X-ray diffractogram of the aluminate precursor Ni-Co.

Again, several diffraction peaks indicate the presence of a spinel phase in this precursor, with a mean crystal size of 22 nm.

Subsequently, after the precursor reduction process, the X-ray diffraction results, indicate that the phases that make up the foams do not undergo any alteration due to the reduction process. However, the observed spinel phase signals disappear and are replaced by numerous signals indicating the presence of Ni and Co metal crystals, as can be seen in the figures below.

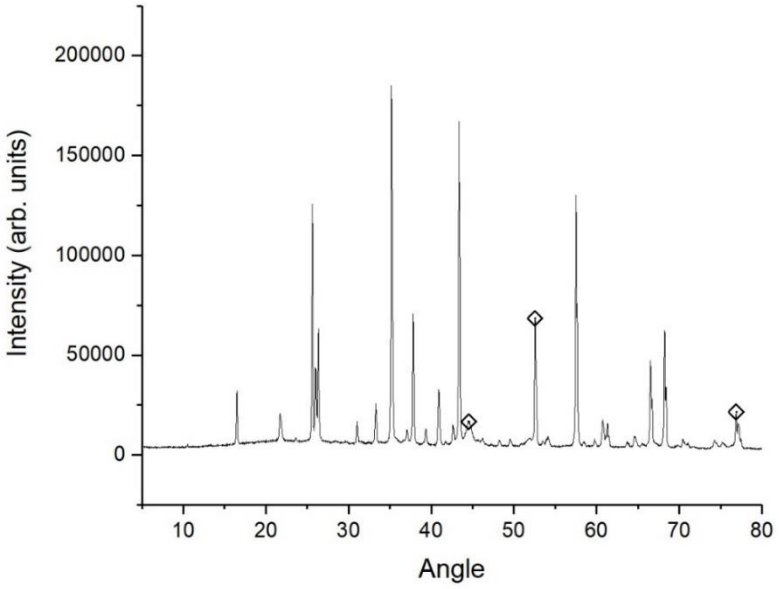

Figure 12.- X-ray diffractogram of the Ni catalyst.

In this case, the Scherrer equation indicates that nickel metallic crystals have an average size of 22 nm.

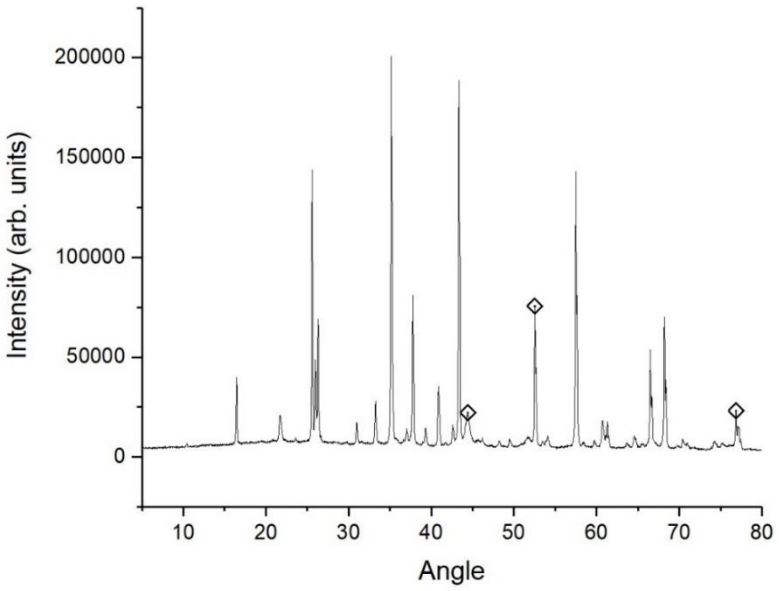

Figure 13.- X-ray diffractogram of the Ni-Co catalyst.

As for nickel-cobalt metal crystals, they had an average size of 24 nm.

The results show that after the reduction, the average size of the crystals increased slightly. The increase in average crystal size after reduction could be due to several factors. During the reduction process, the metal oxides present in the catalyst are reduced to metal metals, which can lead to changes in the structure and morphology of the crystals. First, shrinkage can promote crystal growth through processes such as coalescence, in which smaller crystals join together to form larger crystals. This phenomenon in this case is accentuated by the fact that the reduction process takes place at high temperatures. Second, nucleation and growth of new crystals can occur during reduction. The emergence of new nucleation sites and subsequent crystal growth could contribute to the increase in the average size of crystals in the catalyst.

The increase in crystal size is more pronounced in the case of nickel monometallic catalyst, as the presence of cobalt reduced to metallic form has a stabilizing effect on the size of nickel-cobalt crystals during the reduction process. This phenomenon is explained by the Ostwald effect (Zhang, 2008). The Ostwald effect occurs when smaller particles are dissolved and redeposited into larger particles, after a change in phase or temperature, thus increasing the average size of the crystals over time. Cobalt inhibits this effect because it forms stable alloys with nickel, creating a strong interaction between the two metals. This interaction reduces the mobility of nickel atoms, limiting crystal growth (Jacobs, 2014).

In general, the reduced cobalt-metal form helps maintain a more stable and uniform crystal size in the nickel-cobalt catalyst during reduction, reducing the growth effect of the crystal compared to individual nickel.

9.1.3. Programmed Temperature Reduction with Hydrogen (H2-TPR)

By means of programmed temperature reduction with hydrogen, it is possible to study the redox properties of synthesized catalytic precursors. The TPR profiles are shown in Figure 14.

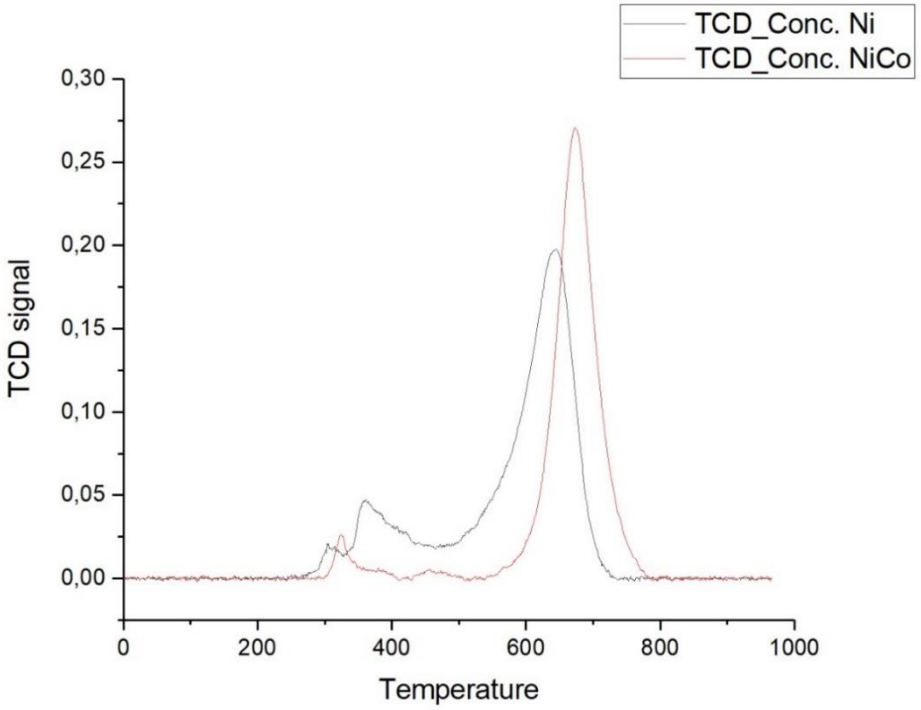

Figure 14.- TPR profiles of catalytic precursors.

A distinction is made between two contributions to hydrogen consumption in catalytic precursors. Firstly, a contribution to low temperatures, i.e. between 350 and 450 °C, which is attributed to the reduction of segregated nickel oxide and segregated cobalt oxide, which react as follows:

$$NiO + H_2 \rightarrow Ni + H_2O \quad (12)$$

$$Co_3O_4 + 4H_2 \rightarrow 3Co + 4H_2O \quad (13)$$

The second contribution, on the other hand, focused on high temperatures, specifically above 550 °C, is attributed to the reduction of nickel aluminate and cobalt aluminate, which react as follows:

$$NiAl_2O_4 + H_2 \rightarrow Ni + Al_2O_3 + H_2O \quad (14)$$

$$CoAl_2O_4 + 4H_2 \rightarrow Co + 2Al_2O_3 + 4H_2O \quad (15)$$

It can be observed that the intensity of the low-temperature contribution is lower for the bimetallic precursor of Ni-Co, which indicates that the incorporation of cobalt promotes the

formation of aluminate spinels, which is also observed by the greater intensity of the high-temperature contribution for the bimetallic precursor.

On the other hand, using the TPR technique it is possible to estimate the percentage of deposited metals that are converted into aluminates. To do this, the total H_2 consumption and H_2 consumption of each phase are calculated using the integration of TPR profiles. So, once the respective consumption has been calculated, it appears that the percentage of nickel converted to aluminate in the monometallic precursor is 78%, while in the case of the nickel-cobalt bimetallic precursor, this percentage rises to 86%. Therefore, cobalt positively influences the formation of nickel aluminate in catalytic precursors.

9.2. RESULTS OF REACTIONS WITHOUT REGENERATION

9.2.1. Catalytic activity of Ni and Ni-Co catalysts

The catalytic activity of nickel and nickel-cobalt foams was studied for the dry methane reforming reaction at 650 °C, for 72 hours. The output current concentration was measured every 0.5 hours. From the measured concentrations, several reaction parameters were determined. Thus, firstly, the evolution of methane and carbon dioxide conversions with reaction time was studied, as well as the H_2/CO molar ratio of the product stream.

First, Figure 15 shows the evolution of reactant conversions for the monometallic nickel catalyst. Thus, it can be seen that the methane and carbon dioxide conversions started at around 40 and 45%, respectively, although the catalyst experienced relatively rapid deactivation during the first 10 hours of reaction, after which its activity stabilized at conversion values around 35 and 40%, respectively.

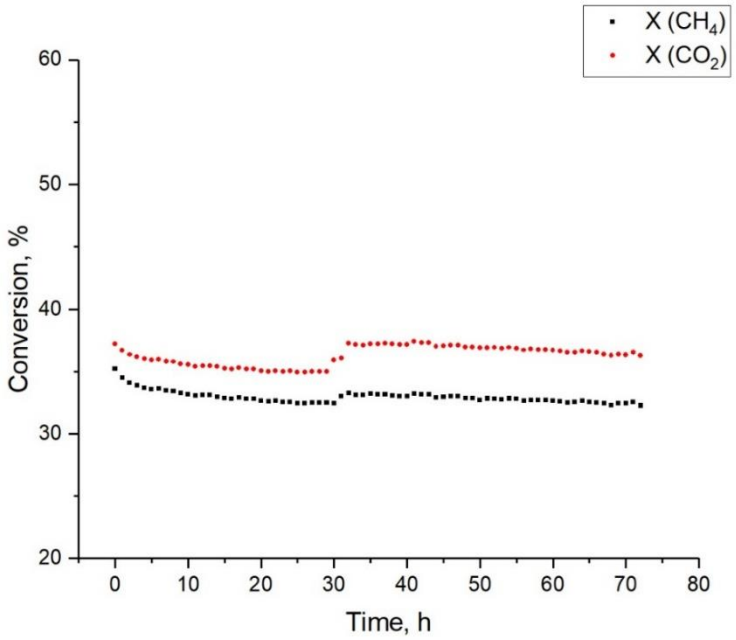

Figure 15.- CH4 and CO2 conversions for the Ni catalyst.

On the other hand, product yields, as shown in Figure 16, followed a similar pattern, with the yield of CO (0.40-0.35) being higher than that of H_2 (0.30-0.25).

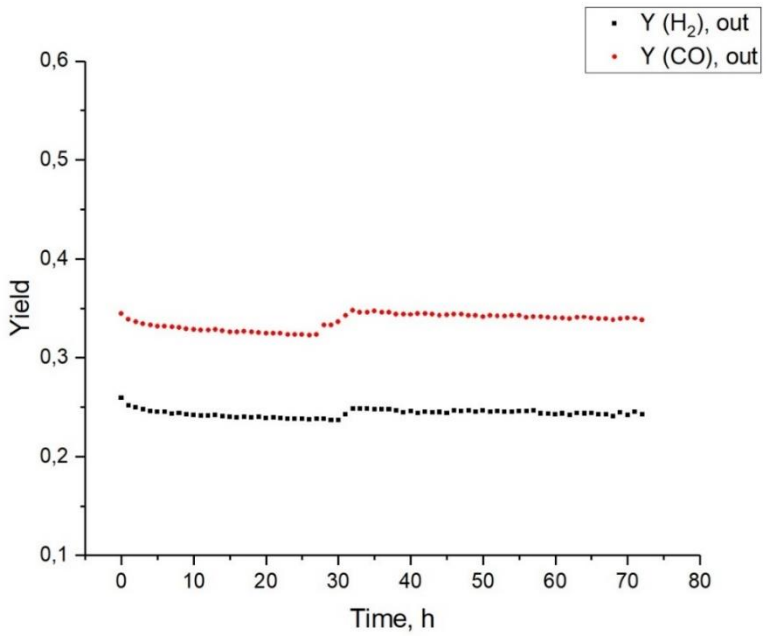

Figure 16.- H_2 and CO yields for the Ni catalyst.

Therefore, as can be seen in Figure 17, the H_2/CO molar ratio was initially 0.72, and then fell to 0.65 towards the end of the reaction. This suggests that initially the DMR reaction occurs more effectively, but then loses efficiency due to parallel reactions. Thus the RWGS reaction tends to consume the hydrogen produced, while the decay of methane and Boudouard reactions form coke, which inhibits the active sites. In practice, after a certain period of time, parallel reactions begin to become more and more frequent, causing the catalyst to lose activity and selectivity to H_2.

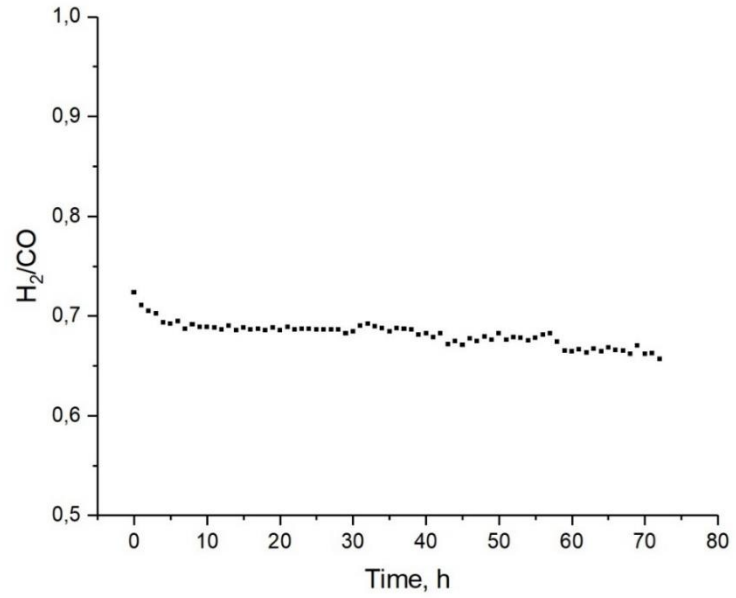

Figure 17.- H2/CO molar ratio for the Ni catalyst.

Subsequently, the reaction was carried out with the Ni-Co catalyst. Under the same operating conditions, the results of the H_2/CO ratio are slightly different.

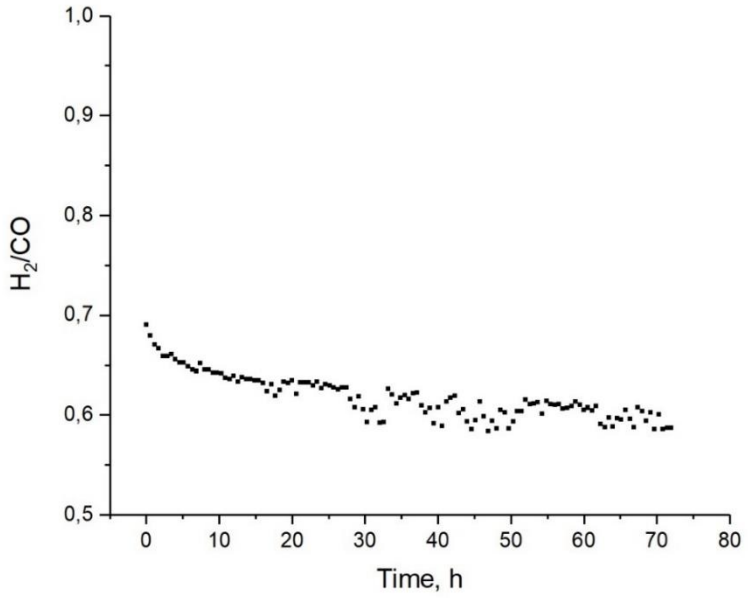

Figure 18.- H2/CO molar ratio for the Ni-Co catalyst.

In this case, the H_2/CO molar ratio is initially 0.69, but then drops to 0.57 at the end of the reaction. In fact, the presence of cobalt seems to give a slightly lower H_2/CO ratio than that of the nickel monometallic catalyst.

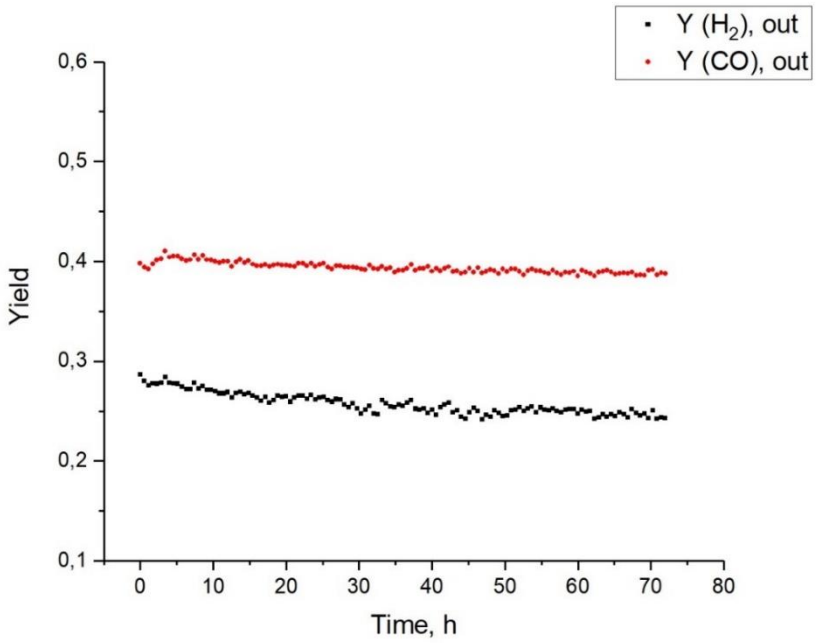

Figure 19.- H2 and CO yields for the Ni-Co catalyst.

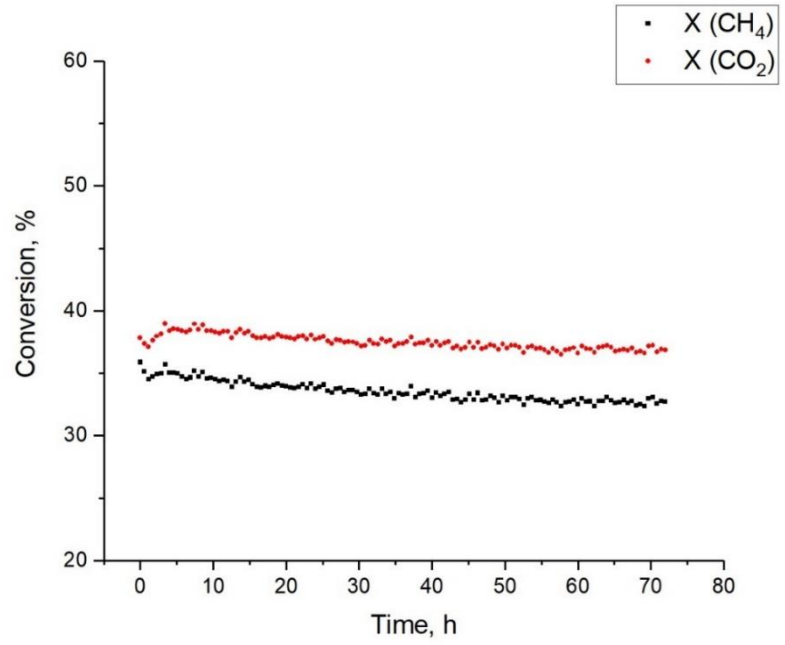

Figure 20.- CH_4 and CO_2 conversions for the Ni-Co catalyst.

Analyzing Figures 19 and 20, it is possible to see that both the conversions of CH_4 and CO_2 and the yields of H_2 and CO follow a stable line. Thus, it can be concluded that cobalt has a stabilizing effect for the DRM reaction and almost manages to inhibit the prevalence of competing reactions due to its higher selectivity compared to monometallic nickel. Therefore, ultimately, cobalt is able to give greater importance to the desired reaction, but suffers a more

marked decrease in H_2/CO yield in comparison. This problem is attributed to the deposition of coke at the active sites of the catalyst (Zhang, 2018).

Since the main problems of the DRM reaction are not only the competitive reactions that reduce the H_2/CO molar ratio, but also the deposition of coke at the active sites of the catalysts, it is necessary to develop a strategy that allows the removal of the coke and, consequently, the regeneration of the active sites of the catalysts (Kim, 2010).

9.2.2. Evaluation of regeneration strategies

At this point, the same reactions are re-studied in different contexts. In fact, in this case the catalyst is regenerated by putting it in contact with 3 different currents in all three cases, i.e. with O_2, with water vapour and with H_2 (Yu, 2020). These regeneration strategies aim for the following coke removal reactions to take place.

With oxygen:

$$C\ (s)\ +\ O_2\ \rightarrow\ CO_2 \tag{16}$$

With water vapor:

$$C\ (s) +\ 2H_2O\ \rightarrow\ CO_2 +\ 2H_2 \tag{17}$$

With hydrogen:

$$C\ (s)\ +\ 2H_2\ \rightarrow\ CH_4 \tag{18}$$

First, we will study the effect of O_2 regeneration on the nickel monometallic catalyst. To carry out this regeneration, a current of 10%O_2/90%N_2 at 650 °C was used for 2 hours, after which the catalyst was subjected to reduction again before continuing with the DRM reaction (Zhou, 2017).

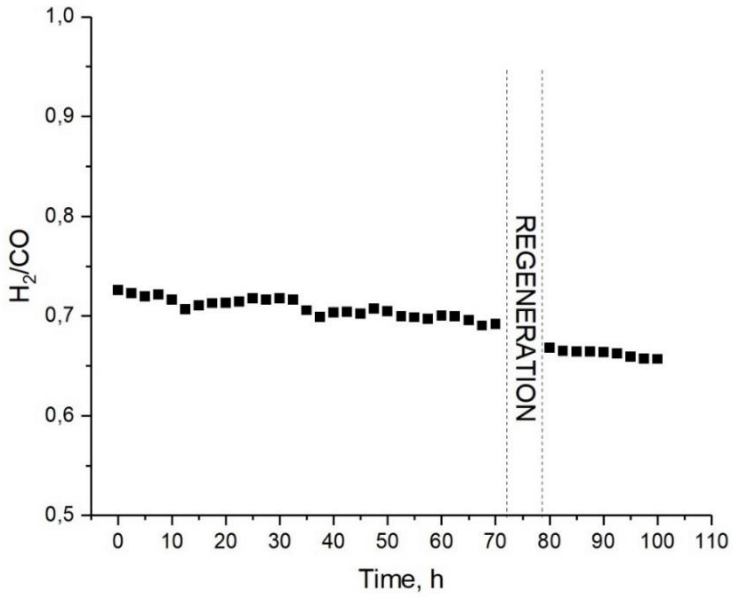

Figure 21.- H_2/CO molar ratio of the Ni catalyst regenerated with O_2.

Figure 21 shows that, after regeneration, the H_2/CO ratio decreased. In fact, removing coke alone is not necessary to increase the H_2/CO ratio, as the reaction is the same.

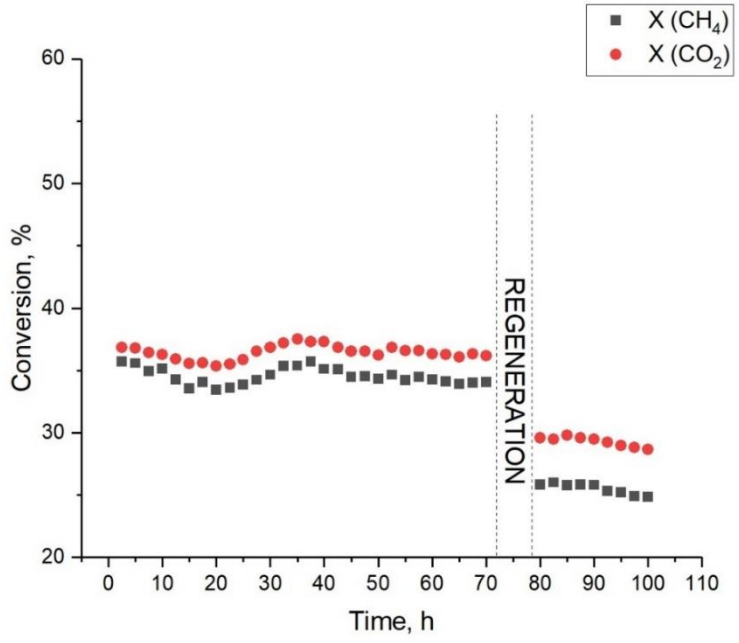

Figure 22.- CH_4 and CO_2 conversions for the O_2-regenerated Ni catalyst.

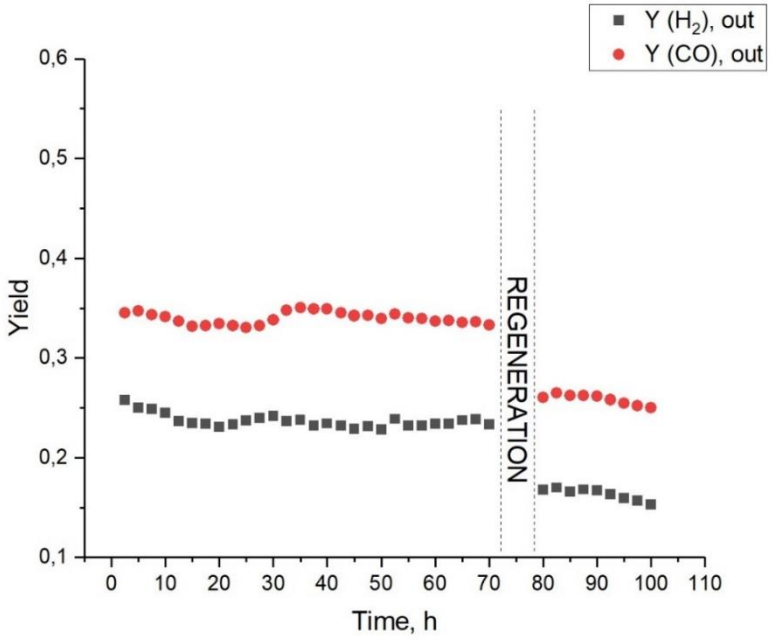

Figure 23.- H_2 and CO yields of the O_2-regenerated Ni catalyst.

Figures 22 and 23 show that not only the H_2/CO ratio is affected by the action of regeneration, but also CO_2 and CH_4 conversions and H_2 and CO yields. Thus, despite the oxygen removing the deposited coke, the regeneration process itself also damages the nickel catalyst, resulting in poorer catalytic behavior after regeneration

On the other hand, the second regeneration strategy consisted of using a mixture of 10%H_2O/90%N_2 at 650 °C for 2 hours. In this case, the coke must react with water vapor to form carbon dioxide and hydrogen.

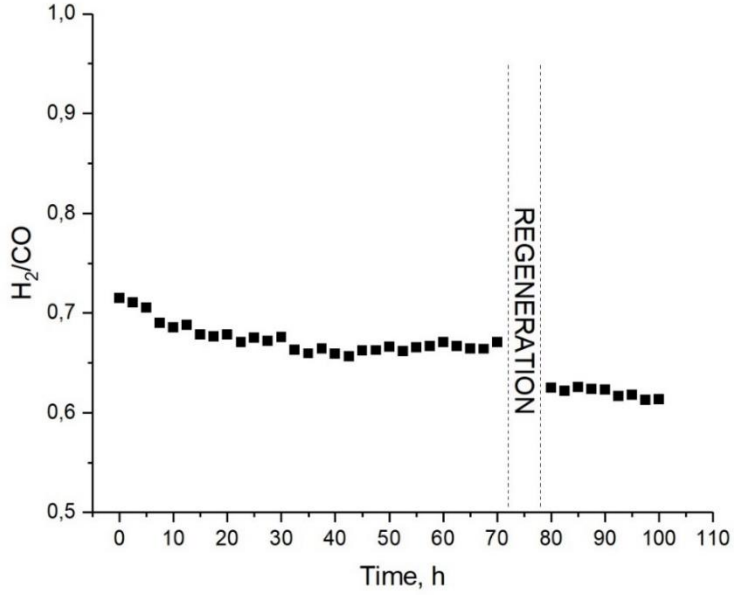

Figure 24.- H_2/CO molar ratio of the Ni catalyst regenerated with H_2O.

Similar to regeneration with O_2, after regeneration, the H_2/CO ratio undergoes a significant reduction.

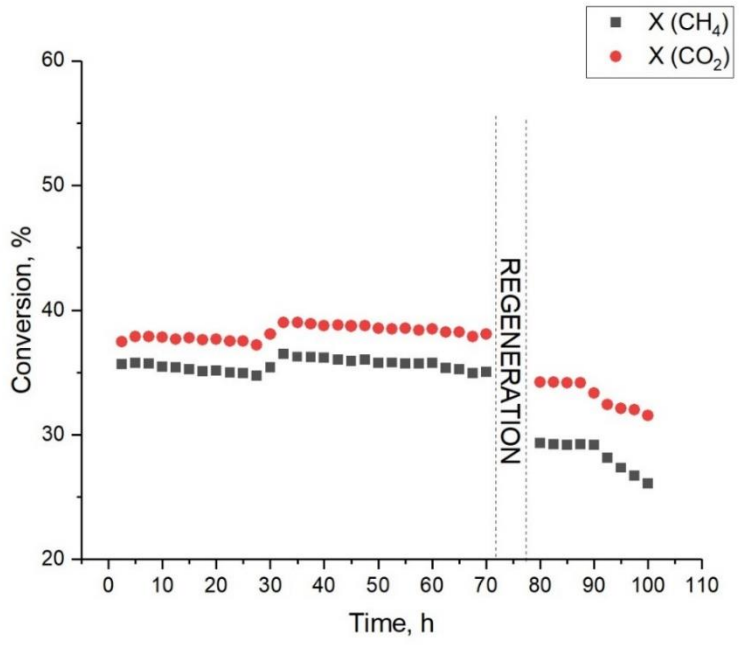

Figure 25.- CH_4 and CO_2 conversions of the Ni catalyst regenerated with H_2O.

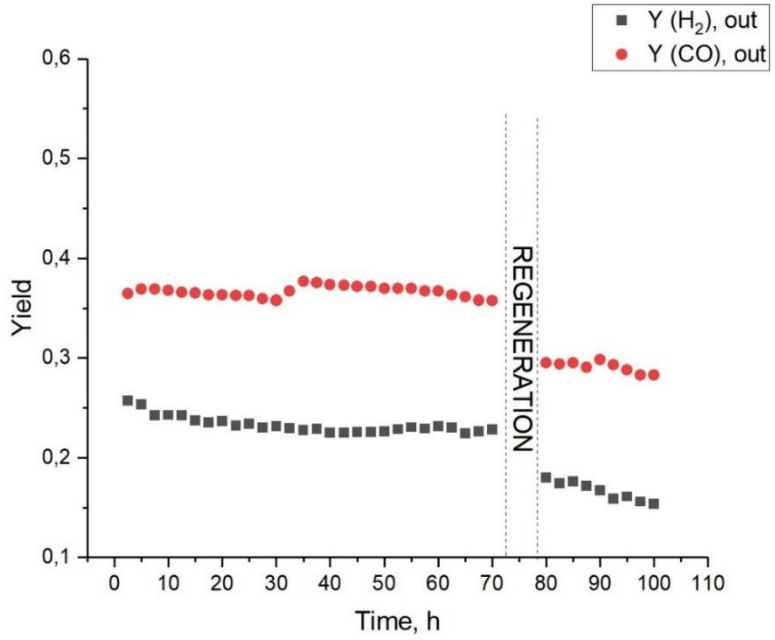

Figure 26.- H_2 and CO yields of the Ni catalyst regenerated with H_2O.

As for the conversions of CO_2 and CH_4 and the yields of H_2 and CO, as can be seen in Figures 25 and 26, they also suffer a significant reduction, although less marked than in the case of oxygen. Based on the results, it can be concluded that this strategy does not contribute to recovering a high reaction efficiency either.

The third regeneration strategy was carried out with a current of 10%H_2/90%N_2 at 650 °C for 2 hours.

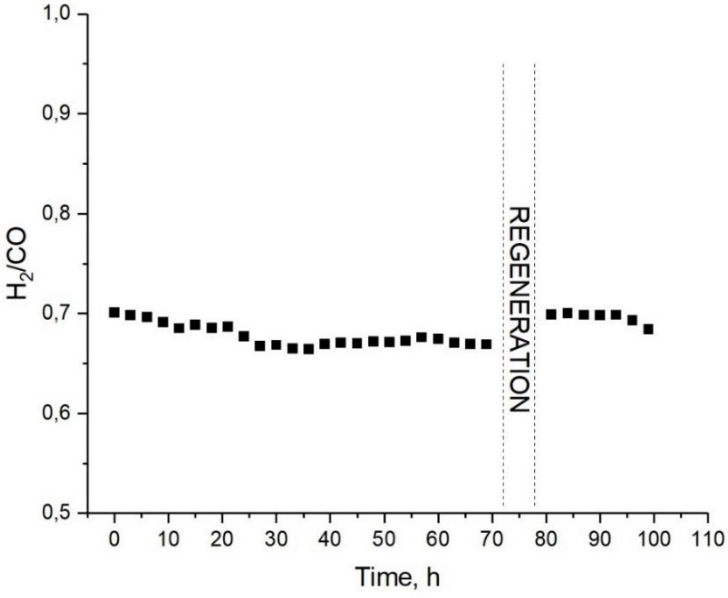

Figure 27.- H_2/CO molar ratio of the Ni catalyst regenerated with H_2.

In Figure 27 it is immediately evident that the H_2/CO ratio has increased after regeneration; This is in contrast to previous regenerations.

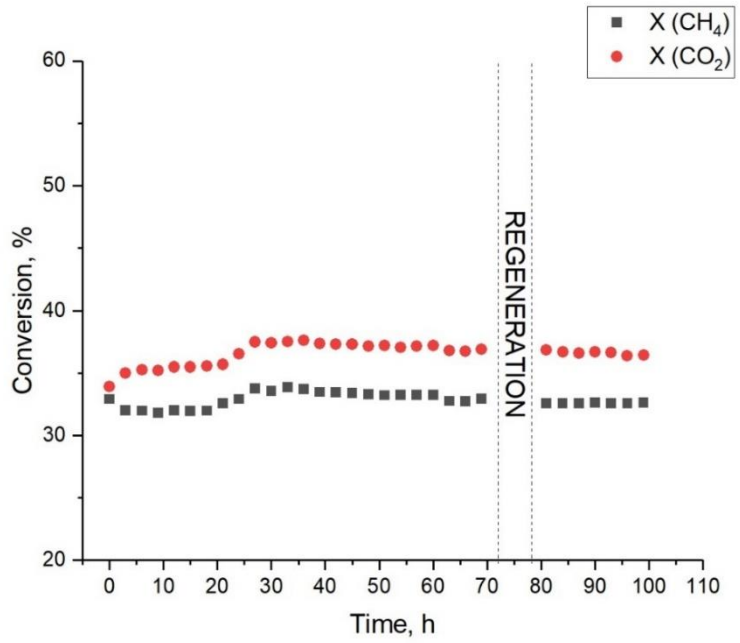

Figure 28.- CH_4 and CO_2 conversions of the Ni catalyst regenerated with H_2.

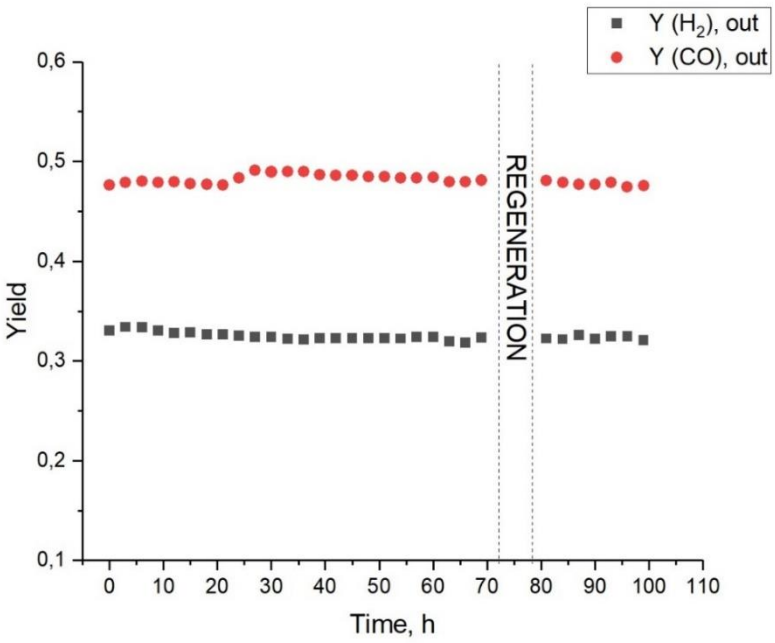

Figure 29.- H_2 and CO yields of the Ni catalyst regenerated with H_2.

With respect to the CO_2 and CH_4 conversions and the H_2 and CO yields shown in Figures 28 and 29, it is observed that, after regeneration, these remained constant. Therefore, it is clear that the utilization of H_2 to regenerate the catalyst does not have the negative effect observed for O_2 and water vapor. The reason for this may be that H_2 allows coke to be removed without reoxidizing the nickel crystals, which prevents them from losing activity.

On the other hand, the effect of the three proposed regeneration strategies on the nickel-cobalt catalyst is studied below. First, the results after regeneration with O_2 are studied.

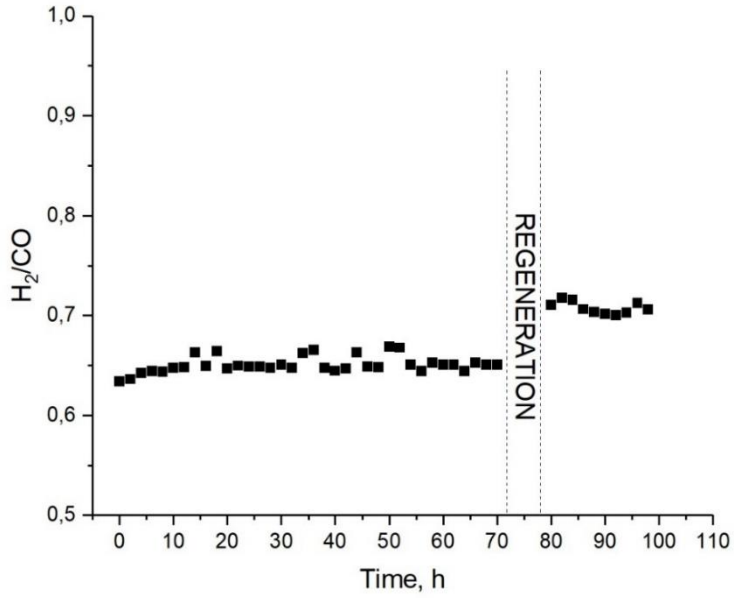

Figure 30.- H_2/CO molar ratio of the Ni-Co catalyst regenerated with O_2.

Figure 30 shows that, after regeneration with O_2, the H_2/CO ratio increases significantly. This may be because the presence of cobalt does not allow nickel reoxidation during regeneration

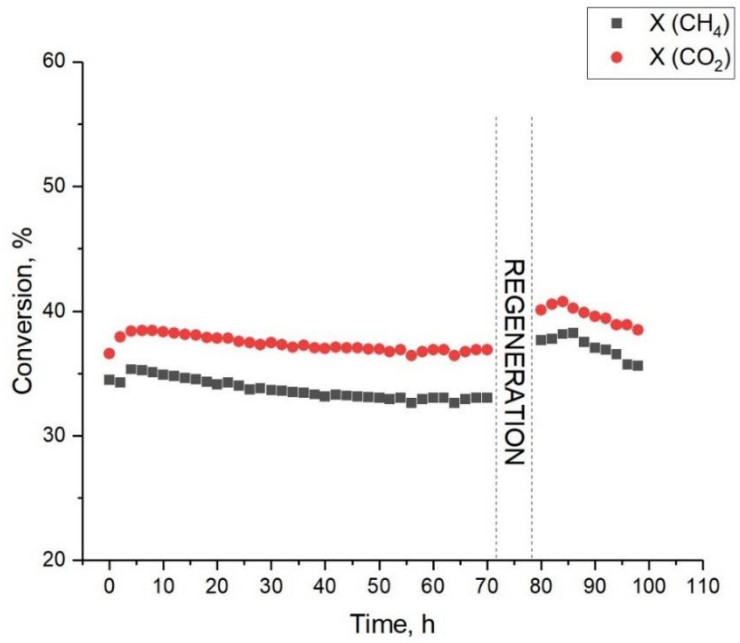

Figure 31.- CH_4 and CO_2 conversions of the Ni-Co catalyst regenerated with O_2.

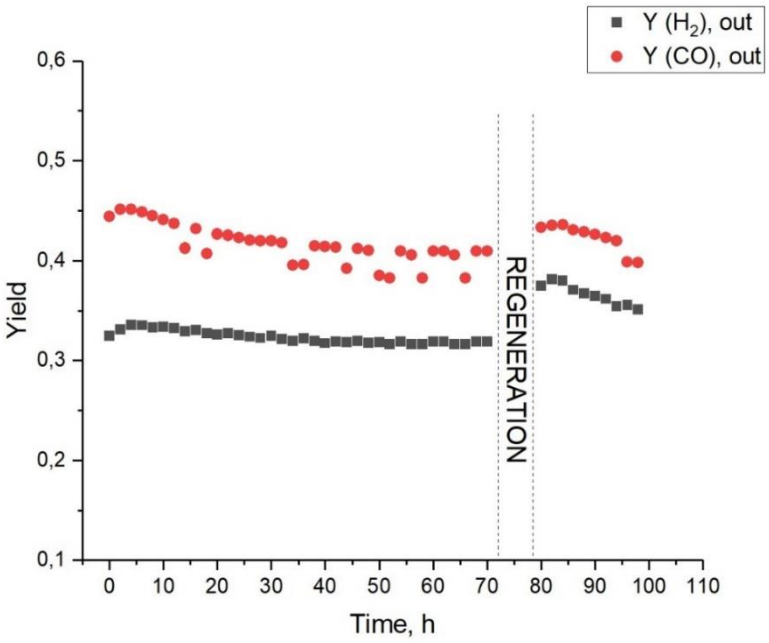

Figure 32.- H_2 and CO yields of the Ni-Co catalyst regenerated with O_2.

Comparing CO_2 and CH_4 conversions and H_2 and CO yields before and after regeneration with O_2, it is observed that both CH_4 conversion and H_2 yield increase significantly. This suggests that the nickel-cobalt catalyst promotes the decay reaction of methane that consumes CH_4 and forms H_2; and that, in addition, the process of regeneration with O_2 and subsequent reduction increases the amount of cobalt available in the catalyst, which improves its activity for the methane decomposition reaction.

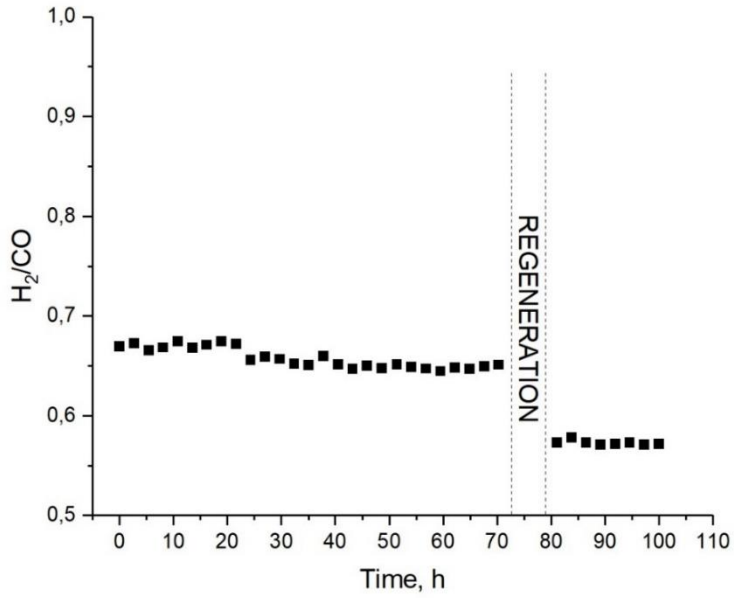

Figure 33.- H_2/CO molar ratio of the Ni-Co catalyst regenerated with H_2O.

On the other hand, as shown in Figure 33, after water vapor regeneration, the H_2/CO molar ratio follows a similar trend to the case of water vapor regeneration of the nickel monometallic catalyst. Thus, the H_2/CO molar ratio declines sharply, probably due to the reoxidation of the catalyst.

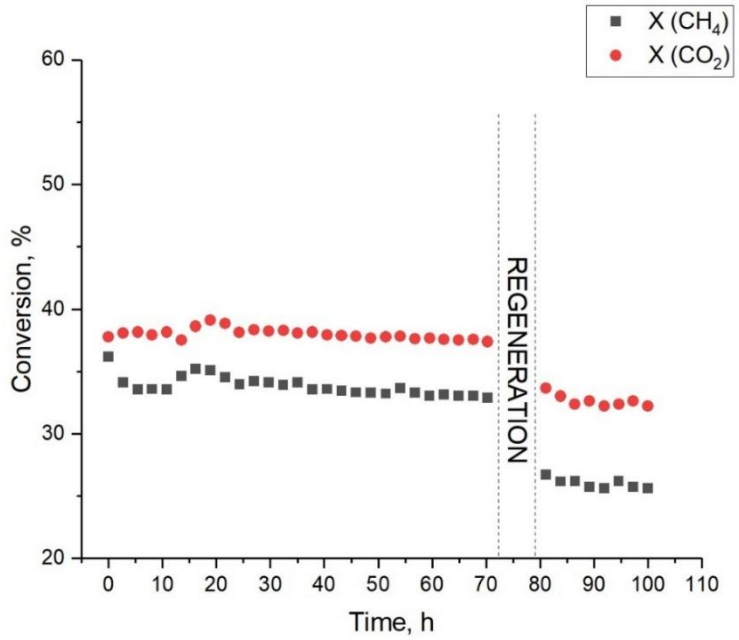

Figure 34.- CH_4 and CO_2 conversions of the Ni-Co catalyst regenerated with H_2O.

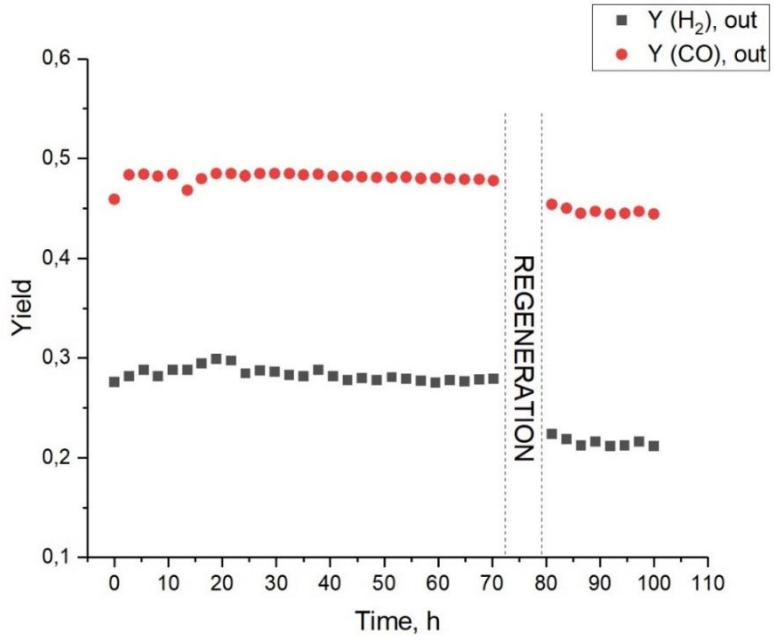

Figure 35.- H_2 and CO yields of the Ni-Co catalyst regenerated with H_2O.

Figures 34 and 35 clearly show a sharp decrease in both CH_4 conversion and H_2 yield. The results obtained for this regeneration strategy suggest that, even in this case, water vapor does not contribute significantly to the removal of coke from active sites and is even less effective than in the case of the nickel monometallic catalyst.

Finally, the effect of regeneration with a flow of hydrogen is studied.

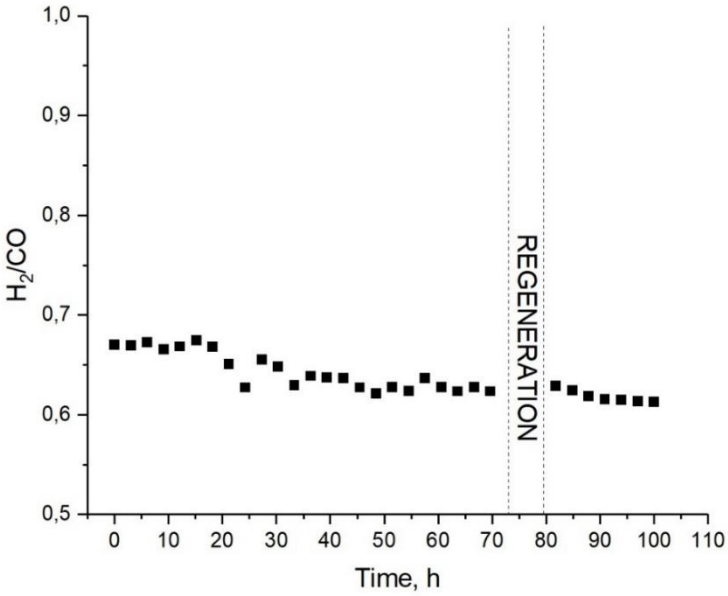

Figure 36.- H_2/CO molar ratio of the Ni-Co catalyst regenerated with H_2.

Figure 36 shows how hydrogen regeneration, in this case, does not increase the H_2/CO molar ratio, which remains stable at around 0.63, suggesting that regeneration with H_2 keeps the properties of the bimetallic catalyst unchanged.

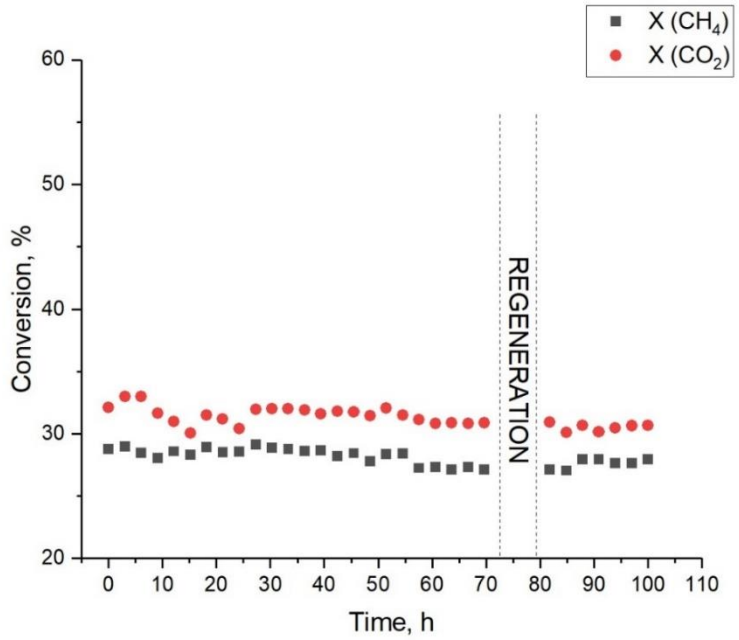

Figure 37.- CH_4 and CO_2 conversions of the Ni-Co catalyst regenerated with H_2.

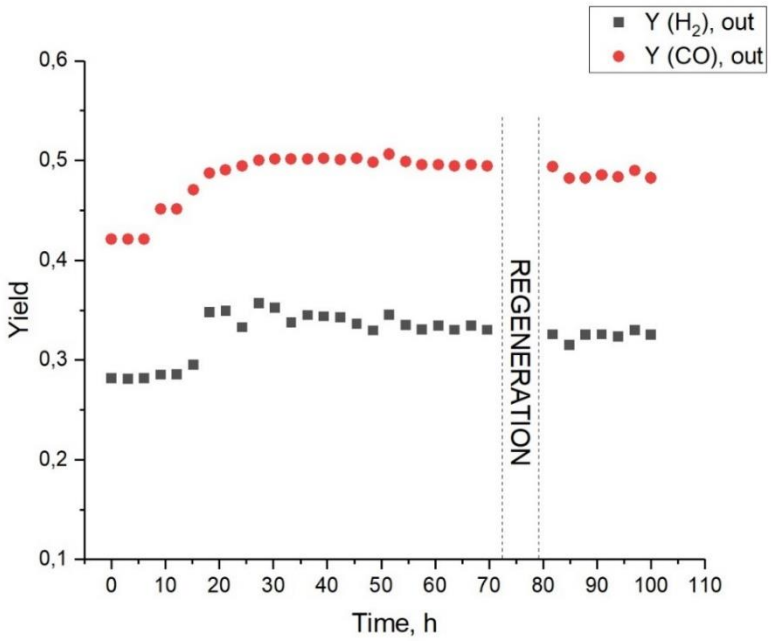

Figure 38.- H_2 and CO yields of the Ni-Co catalyst regenerated with H_2.

As shown in Figures 37 and 38, similar to the nickel monometallic catalyst, the reaction parameters remain constant after regeneration.

Finally, if we compare the molar H_2/CO ratio of the syngas produced by the nickel monometallic catalyst in the three regeneration strategies studied, we obtain the results represented in Figure 39.

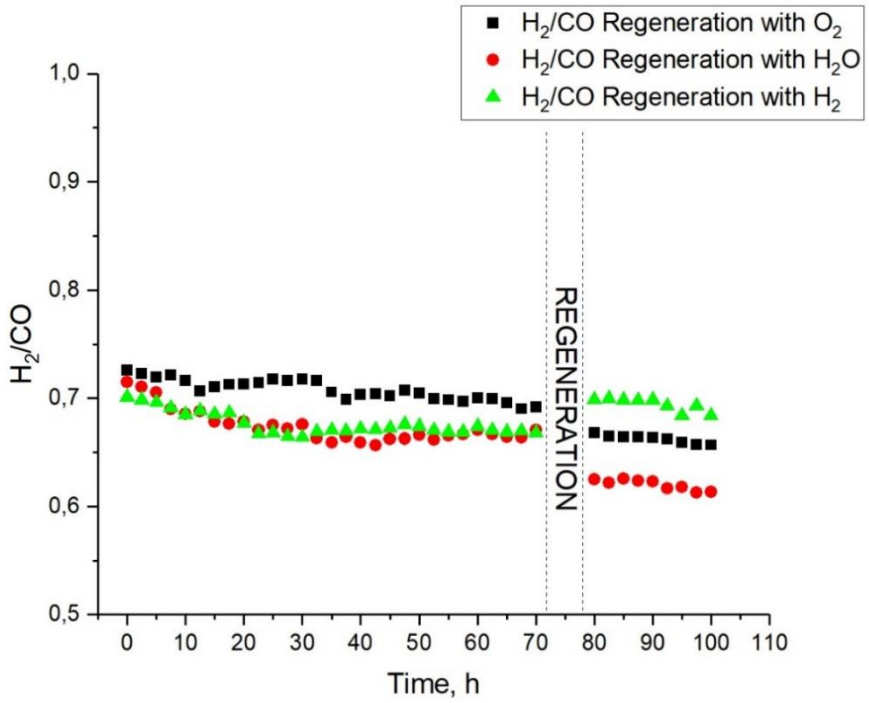

Figure 39.- Comparison of the H_2/CO molar ratio of the Ni catalyst for the three regeneration strategies studied.

The results shown in Figure 39 show that, in the case of the nickel monometallic catalyst, only with regeneration with H_2 leads to an increase in the molar ratio of H_2/CO, while the other two strategies studied contribute to reduce the selectivity to H_2 of the catalyst.

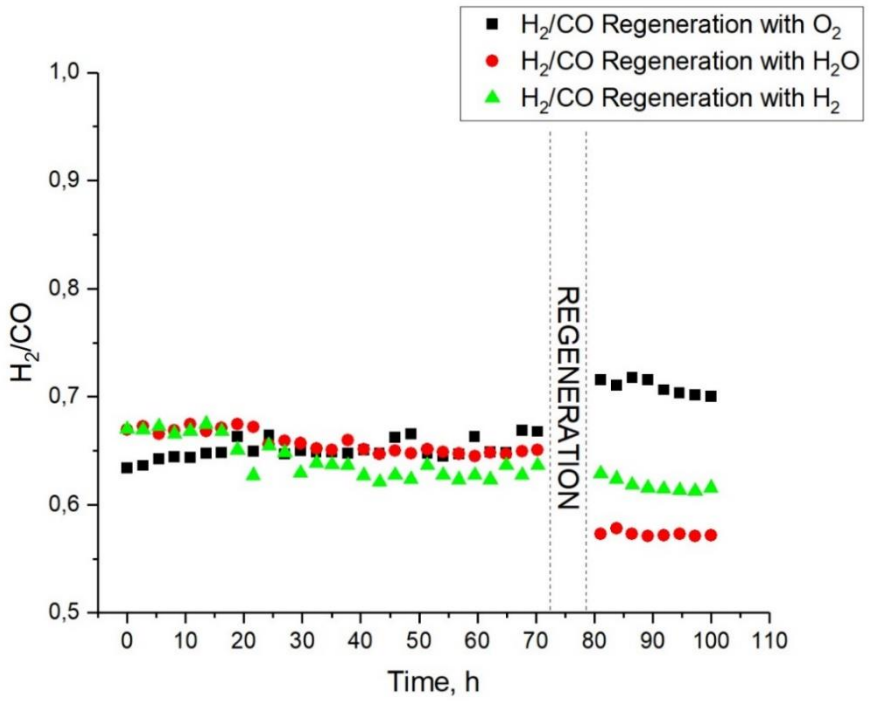

Figure 40.- Comparison of the H_2/CO molar ratio of the Ni-Co catalyst for the three regeneration strategies studied.

On the other hand, the results in Figure 40 clearly indicate that the H_2/CO molar ratio only increases when the Ni-Co bimetallic catalyst is regenerated using O_2. In both cases, it has been observed that water vapor regeneration is clearly harmful to the catalysts studied.

10. CONCLUSIONS

The behavior of nickel and nickel-cobalt catalysts after the regeneration process showed significant differences due to the intrinsic chemical properties of the two metals. Cobalt, with its high affinity for oxygen, tends to form stable oxides (such as CoO or Co_3O_4), facilitating carbon oxidation reactions. These reactions, being highly exothermic and thermodynamically favorable for methane formation, make cobalt an effective catalyst for such processes. On the other hand, nickel is highly selective in methanation catalysis, thanks to its ability to efficiently adsorb and dissociate hydrogen and carbon molecules on its surface. This enables the formation of methane through stable intermediates such as CHx.

In the context of catalyst regeneration, experimental results showed that in the case of pure nickel, regeneration with hydrogen led to an increase in the H_2/CO ratio, indicating an effective restoration of nickel's active sites for methanation. However, regeneration with oxygen resulted in a decrease in this ratio due to the formation of nickel oxides, which can poison active sites, reducing nickel's ability to catalyze coke oxidation. Conversely, for the nickel-cobalt catalyst, the H_2/CO ratio remained nearly constant when regenerated with hydrogen. This suggests that cobalt prevented the complete restoration of nickel's active sites, maintaining a stable equilibrium between reaction products. On the other hand, when the nickel-cobalt catalyst was regenerated with oxygen, the H_2/CO ratio increased significantly due to cobalt's strong affinity for oxygen, the reduction process, and the competition between nickel and cobalt for active sites, allowing greater availability of carbon in the form of coke for CO_2 formation.

Given these findings, optimizing catalyst regeneration conditions is crucial to improving efficiency and durability. One possible approach to mitigate the formation of undesired oxides and maximize methanation selectivity could involve advanced controlled reduction techniques, such as hydrogen plasma-assisted treatment or selective microwave heating. These methods could allow for more precise regeneration by reducing oxides in a controlled manner while preserving the integrity of active sites.

Additionally, integrating innovative catalytic supports, such as mixed oxides, graphene-based materials, modified zeolites, or destabilized cerium oxides, could enhance the dispersion of nickel and cobalt, limiting their tendency toward oxidation and improving thermal stability. Recent studies have demonstrated that nanostructured supports can contribute to more effective regeneration by confining metals in well-defined active sites, preventing deactivation (Cappelli, 2023).

Another relevant aspect for future research concerns the development of co-regeneration strategies under dynamic conditions, where the regeneration atmosphere is modulated in real time based on the catalyst's state. In-situ spectroscopy techniques could provide detailed insights into the chemical composition of active sites during regeneration, enabling more precise adaptation of the reduction strategy.

Finally, the exploration of binary or ternary alloys containing nickel, cobalt, and other transition metals (such as iron or copper) could open new avenues for designing catalysts with higher resistance to poisoning and improved regenerability. The synergy between these metals could lead to a more uniform distribution of active sites and greater flexibility in regeneration processes, contributing to higher and more sustainable yields.

In conclusion, future research should focus on optimizing regeneration conditions through innovative reduction techniques, the use of advanced supports, and intelligent co-regeneration strategies. Moreover, the exploration of new catalytic materials could offer further improvements in stability and efficiency, making methanation processes increasingly reliable and sustainable for large-scale industrial applications.

11. BIBLIOGRAPHY

Abdullah B., Ghani, N. A. A., & Vo, D. V. N. (2017). Recent advances in dry reforming of methane over Ni-based catalysts. Journal of Cleaner Production, 162, 170-185. https://doi.org/10.1016/j.jclepro.2017.05.176

Armor J. N. (1999). The multiple roles for catalysis in the production of H2. Applied Catalysis A: General, 176(2), 159-176. https://doi.org/10.1016/S0926-860X(98)00254-4

Arrhenius (1896). On the influence of carbonic acid in the air upon the temperature of the ground. Philosophical Magazine and Journal of Science, 41(5), 237-276.

Balasubramanian B., Ortiz Vega, D., Kaytakoglu, S., & Harrison, D. P. (1999). Hydrogen from methane in a single-step process. Chemical Engineering Science, 54(15-16), 3543-3552. https://doi.org/10.1016/S0009-2509(99)00098-0

Bragg W.H., & Bragg, W.L. (1913). *The Reflection of X-rays by Crystals*. Proceedings of the Royal Society of London. Series A, Containing Papers of a Mathematical and Physical Character, 88(605), 428-438.

Cappelli, C., et al. (2023). *Nigraf: A graphene-based catalyst for enhanced hydrogen production.* Rinnovabili.it. https://www.rinnovabili.it/mercato/rd/catalizzatore-grafene-cnr/

Carbos R. A., et al. (2018). Solution Combustion Synthesis of Catalysts: Principles and Applications. *Journal of Catalysis*, 365, 117-133.

Chen L., et al. (2023). "*Atomic-Level Design and Synthesis of Cobalt-Based Catalysts for Efficient Dry Reforming of Methane.*" *ACS Nano*, 17(1), 558-571.

Chin Y.H., et al. (1993). *Temperature-Programmed Reduction Studies of Nickel Oxide/Alumina Catalysts*. Journal of Catalysis, 139(2), 446-460.

Choi S., & Stenger, H. G. (2003). Water gas shift reaction kinetics and reactor modeling for fuel cell grade hydrogen. Journal of Power Sources, 124(2), 432-439. https://doi.org/10.1016/S0378-7753(03)00773-6

Ciambelli et al. (2009). Comparison of ceramic honeycomb monolith and foam as Ni catalyst carrier for methane autothermal reforming. Catalysis Today, 155 (2010), 92-99. http://dx.doi.org/10.1016/j.cattod.2009.01.021

Davis B. H. (2003). "Fundamentals of Chemical Reaction Engineering." McGraw-Hill.

De Smet S., Marin, G. B., & Waroquier, M. (2001). Ab initio study of the reactions of CH4 with CO2 and H2O over a Ni(111) surface. Journal of Physical Chemistry B, 105(24), 5345-5351. https://doi.org/10.1021/jp004455d

Ertl, G., Knözinger, H., & Weitkamp, J. (Eds.). (2008). "Preparation of Solid Catalysts." In *Handbook of Heterogeneous Catalysis* (2nd ed., pp. 1012-1024). Wiley-VCH.

Gallucci F., Basile, A., & Tosti, S. (2008). Methane dry reforming over nickel membrane reactor: The effect of catalytic activity and membrane permeation. International Journal of Hydrogen Energy, 33(16), 4456-4462. https://doi.org/10.1016/j.ijhydene.2008.05.018

Gibb H. J., et al. (July 7, 2000). Lung cancer among workers in chromium chemical production. *American Journal of Industrial Medicine* (*AJIM)* 38.2:115-126. Describes a study regarding the incidence of lung cancer among workers in chromium chemical production.

Gielen D., Boshell, F., Saygin, D., Bazilian, M. D., Wagner, N., & Gorini, R. (2019). The role of renewable energy in the global energy transformation. Energy Strategy Reviews, 24, 38-50.

Goulas A., et al. (2017). "In Situ Spectroscopic Studies on the Oxidation States of Chromium in Ni-Cr Catalysts During Dry Reforming of Methane." *ACS Catalysis*, 7(8), 5184-5196.

Hoffert M. I., Caldeira, K., Benford, G., Criswell, D. R., Green, C., Herzog, H., & Wigley, T. M. L. (2002). Advanced technology paths to global climate stability: Energy for a greenhouse planet. Science, 298(5595), 981-987.

IEA (International Energy Agency) (2020). World energy outlook 2020. Paris: IEA Publications.

IPCC (Intergovernmental Panel on Climate Change) (2014). Climate change 2014: Synthesis report. Contribution of Working Groups I, II, and III to the Fifth Assessment Report of the Intergovernmental Panel on Climate Change. Geneva, Switzerland: IPCC.

Jacobs G., Wenping Ma and Burtron H. Davis, (2014). Influence of Reduction Promoters on Stability of Cobalt/γ-Alumina Fischer-Tropsch Synthesis Catalysts. Catalysts, 50-53

Karpe S., Götz Veser (2024). "Coke Formation and Regeneration during Fe-ZSM-5-Catalyzed Methane Dehydro-Aromatization." Catalysts, 14(5), 292.

Kim Y. H., et al. (2010). "Catalytic behavior of supported cobalt catalysts in the dry reforming of methane." *Applied Catalysis A: General*, 391(1-2), 158-163.

Knözinger H., J. Weitkamp (eds.) (2008). "Handbook of Heterogeneous Catalysis." Wiley-VCH.

Matus E. V., Al-Muhtaseb, S. A., & Cox, H. W. (2012). Recent advancements in catalytic materials for methane dry reforming: A review. Energy & Fuels, 26(7), 4194-4219. https://doi.org/10.1021/ef300223a

Leung D. Y. C., Leung, M. K. H., & Sumathy, K. (2007). Dry reforming of methane: A critical review on the reaction mechanism, catalysts development, and process design. Renewable and Sustainable Energy Reviews, 11(3), 401-425. https://doi.org/10.1016/j.rser.2005.01.006

Murthy K. K., & Maiti, H. S. (2002). Hydrogen production by partial oxidation of methane: A review. International Journal of Hydrogen Energy, 27(10), 1061-1070. https://doi.org/10.1016/S0360-3199(02)00026-6

NAS (National Academy of Sciences) (1979). Understanding climate change: An agenda for action. Washington, DC: National Academy Press.

Navarro R. M., Peña, M. A., & Fierro, J. L. G. (2007). Hydrogen production reactions from carbon feedstocks: Fossil fuels and biomass. Chemical Reviews, 107(10), 3952-3991. https://doi.org/10.1021/cr0501994

Patterson A.L. (1939). *The Scherrer Formula for X-Ray Particle Size Determination*. Physical Review, 56, 978-982.

Rostrup-Nielsen, J. R. (1984). Catalysis: Science and Technology (Vol. 5). Berlin, Germany: Springer. DOI:10.1007/978-3-642-93214-8

Rostrup-Nielsen J. R., Sehested, J., & Nørskov, J. K. (2002). "Hydrogen and synthesis gas by steam- and C02 reforming." *Advances in Catalysis*, 47, 65-139.

Rostrup-Nielsen J. R., & Christiansen, L. J. (2011). Concepts in Syngas Manufacture. London, England: Imperial College Press. https://doi.org/10.1142/p726

Rouibah K., et al. (2017). Dry reforming of methane on nickel-chrome, nickel-cobalt and nickel-manganese catalysts. International Journal of Hydrogen Energy, 1-9 https://doi.org/10.1016/j.ijhydene.2017.10.049

Saruhan O., M. Luginsland, A. Naoumidis, H. Nickel (1996). Reaction and Sintering Mechanisms of Mullite in the Systems Cristobalite/Alpha-Al2O3 and Amorphous SiO2/Alpha-Al2O3. Journal of the European Ceramic Society, 16, 413-421.

Solomon S., Plattner, G.-K., Knutti, R., & Friedlingstein, P. (2009). Irreversible climate change due to carbon dioxide emissions. Proceedings of the National Academy of Sciences, 106(6), 1704-1709.

Song, C. (2006). Global challenges and strategies for control, conversion and utilization of CO2 for sustainable development involving energy, catalysis, adsorption and chemical processing. Catalysis Today, 115(1-4), 2-32. https://doi.org/10.1016/j.cattod.2006.02.029

Specchia S., Italiano C., Ashraf A. M., Pino L. (2018). Rh/CeO2 Thin Catalytic Layer Deposition on Alumina Foams: Catalytic Performance and Controlling Regimes in Biogas Reforming Processes. Catalysts.

Specchia S., Galletti C., Specchia V. (2010). Solution Combustion Synthesis as intriguing technique to quickly produce performing catalysts for specific applications. 10th International Symposium “Scientific Bases for the Preparation of Heterogeneous Catalysts”.

Specchia S., Vita A., Italiano C., Ashraf A. M., Pino L. (2017). Syngas production by steam and oxy-steam reforming of biogas on monolith-supported CeO2-based catalysts. International Journal of Hydrogen Energy 43.

Sun Y., Y. Zhang, X. Yin, C. Zhang, Y. Li and J. Bai, (2024). Recent advances in the design of high performance cobalt based catalyst for dry reforming of methane. Green Chemistry, 1-2. DOI: 10.1039/D3GC05136F.

Taylor T. E., S. A. Speakman, D. J. Mackenzie (2016). Formation and Structure of Cordierite Ceramic Foam. Journal of the European Ceramic Society, 36(10), 2547-2555.

Ukhurebor et al. (2021). Effect of hexavalent chromium on the environment and removal techniques: A review. Journal of Environmental Management (280), 2-4.

UNFCCC (United Nations Framework Convention on Climate Change) (2015). Paris Agreement. Retrieved from [UNFCCC website] (https://unfccc.int/process-and-meetings/the-paris-agreement/the-paris-agreement).

Wang Q., et al. (2022). "Advances in Co-based Catalysts for Dry Reforming of Methane: From Fundamentals to Applications." *Catalysis Science & Technology*, 12(3), 935-953.

Wang S., & Lu, G. Q. (1998). "Role of CeO2 in Ni/CeO2–Al2O3 catalysts for carbon dioxide reforming of methane." *Applied Catalysis B: Environmental*, 16(3-4), 269-277.

Wang S., & Lu, G. Q. (2000). Reforming of methane with carbon dioxide over Ni/Al2O3 catalysts: Effect of nickel precursor. Applied Catalysis B: Environmental, 16(3), 269-277. https://doi.org/10.1016/S0926-3373(97)00105-4

Wang W., Zhang, X., & Zhang, L. (2012). Advances in catalytic dry reforming of methane. Chinese Journal of Catalysis, 33(6), 967-980. https://doi.org/10.1016/S1872-2067(11)60358-0

Xie Yanling, Rong Xu, Bi Sheng (2014). "*Application, Deactivation, and Regeneration of Heterogeneous Catalysts in Bio-Oil Upgrading.*" Catalysts, 4(2), 77-93.

Yu, X., et al. (2020). "Effect of O2 regeneration on the performance of Ni-based catalysts in dry reforming of methane." *Chemical Engineering Journal*, 382, 122956.

Zhang H., Chuanxin Zhai, Jianbo Wu, Xiangyang Ma and Deren Yang, (2008). Cobalt ferrite nanorings: Ostwald ripening dictated synthesis and magnetic properties. Chemical communications, 5648-5650.

Zhang, Y., et al. (2018). "Cobalt catalysts for dry reforming of methane." *Chemical Engineering Journal*, 333, 108-122.

Zhou, S., et al. (2017). "Effect of O2 regeneration on the structure and performance of Ni-based catalysts for CO2 reforming of methane." *Applied Catalysis B: Environmental*, 207, 254-263.

Zhu, J., et al. (2010). "Review of Ni-based catalysts for dry reforming of methane." *Catalysis Today*, 178(1), 76-87.